

PCAMM 2022 Poster Program

University of Victoria

December 10, 2022



**University
of Victoria**

Centre for
Advanced Materials
& Related Technology

Lipid Nanoparticle Mediated Delivery of Docetaxel Prodrug for Exploiting Full Potential of Gold Radiosensitizers in the Treatment of Pancreatic Cancer

Abdulaziz Alhussan¹, Nolan Jackson¹, Nancy Dos Santos², Ingrid Barta³, Josh Zaifman⁴, Sam Chen⁴, Yuen Yi CTam⁴, Sunil Krishnan⁵, Devika B Chithrani^{1,6,7, 8, 9,10*}

¹ Department of Physics and Astronomy, University of Victoria, Victoria, BC V8P 5C2, Canada

² Department of Experimental Therapeutics, British Columbia Cancer-Vancouver, Vancouver, BC V5Z 1L3, Canada

³ Centre for Comparative Medicine, Animal Care Services, University of British Columbia, Vancouver, BC V6T 1W5, Canada

⁴ Integrated Nanotherapeutics Inc., Burnaby, BC V5G 4X4, Canada

⁵ Department of Radiation Oncology, Mayo Clinic, Jacksonville, FL 32224, USA.

⁶ Radiation Oncology, British Columbia Cancer-Victoria, Victoria, BC V8R 6V5, Canada

*Correspondence: devikac@uvic.ca

Pancreatic cancer is one of the leading causes of cancer deaths worldwide. Current chemoradiation therapy suffers from normal tissue toxicity. To overcome this problem, we are proposing incorporating nanoparticles as radiosensitizers and as drug delivery vehicles into current chemoradiation regimes. Gold nanoparticles (GNPs) and Docetaxel (DTX) have shown very promising synergetic radiosensitization effects despite DTX toxicity to normal tissues. In this experiment, we explored the effect of DTX prodrug encapsulated in lipid nanoparticles (LNP_{DTX-P}) on GNP uptake in pancreatic cancer models *in vitro* and *in vivo*. For the *in vitro* experiment, the pancreatic cancer cell line, MIA PaCa-2, was cultured and dosed with 7.5 µg/mL of GNPs (of ~ 11 nm in diameter functionalized with PEG and RGD peptide) and with 45 nM of free DTX or equivalent dose of LNP_{DTX-P}. For the *in vivo* experiment, MIA PaCa-2 were implanted subcutaneously in NRG mice and the mice were dosed with 2 mg/kg of GNPs and 6 mg/kg of DTX or an equivalent dose of LNP_{DTX-P}. GNPs content in mice and in cells was measured using Inductively Coupled Plasma–Mass Spectrometry (ICP–MS). The results show that LNP_{DTX-P} treated tumour samples 191% increase in GNPs uptake compared to control samples in both *in vitro* and *in vivo*. The results also show that LNP_{DTX-P} treated tumour samples have retained over 160% of GNPs compared to control samples in both *in vitro* and *in vivo*. No significant difference was found in GNP uptake or retention between free DTX and LNP_{DTX-P} in tumour-treated samples *in vivo*. The results are very promising as LNP_{DTX-P} have superior targeting of tumour tissues compared to free DTX due to their nano size and their ability to be functionalized. Because of their minimal toxicity to normal tissues, both GNPs and LNP_{DTX-P} can be ideal radiosensitization candidates in radiotherapy and would produce very promising synergistic therapeutic outcomes. Current radiotherapy treatments can hugely benefit from the effects of these two radiosensitizers boosting the radiation dose to the tumour while reducing the normal tissue dose. This in return will improve patient outcomes and quality of life.

This work was supported by the University of British Columbia, BC Cancer (Vancouver & Victoria), Integrated Nanotherapeutics Inc, Kuwait Foundation for the Advancement of Sciences (KFAS) under project code CB21-63SP-01, Nanomedicines Innovation Network Strategic Initiative fund (NMIN-SI), the John R. Evans Leaders Fund (JELF) from the Canada Foundation for Innovation (CFI) and British Columbia Knowledge Development Fund (BCKDF), the NSERC Discovery grant from the Natural Sciences and Engineering Research Council of Canada (NSERC), collaborative health grant from the University of Victoria, and grants code R01CA257241, R01DE028105, R21CA252156 and R01CA274415 from the National Institutes of Health (NIH) of United States of America.

Tensor network methods for materials in the DMRjulia library

T.E. Baker^{1,2,3,*}

¹University of Victoria, Department of Physics & Astronomy

²University of Victoria, Department of Chemistry

³Centre for Advanced Materials and Related Technologies

e-mail: bakerte@uvic.ca

Tensor network simulations are a highly efficient solver for one-dimensional quantum systems. They also perform well for long-range interactions and higher-dimensional models. A new library, DMRjulia is fast and efficient and easy to use. Programming in the Julia language, which is a Python-like language but faster, allows for students to complete projects on a reasonable time-scale but with a code that can outperform lower-level implementations. Thorough documentation ensures complete transparency with all developments. Recent implementations into the code deal with *ab initio* computations for quantum chemistry systems. I cover the capabilities and power of the library while pursuing new directions with the code.

This research was undertaken, in part, thanks to funding from the Canada Research Chairs Program. The Chair position in the area of Quantum Computing for Modeling of Molecules and Materials is hosted by the Departments of Physics & Astronomy and of Chemistry at the University of Victoria. T.E.B. is grateful for support from the University of Victoria's start-up grant from the Faculty of Science.

References

- [1] T.E. Baker, S. Desrosiers, M. Tremblay, M.P. Thompson, *Canadian Journal of Physics*, **99**, 4 (2021).
- [2] T.E. Baker and M.P. Thompson, *arxiv: 2109.03120*.
- [3] T.E. Baker, et. al., *arxiv: 2111.14530*.
- [4] T.E. Baker, DMRjulia: github.com/bakerte/DMRJtensor.jl

Length-Controlled Nanofiber Micelleplexes as Efficient Nucleic Acid Delivery Vehicles

S. T. G. Street,^{1,2,3} J. Chrenek,^{4,5} R. L. Harniman,¹ K. Letwin,^{4,5} S. M. Willerth,^{3,4,5} I. Manners^{1,2,*}

¹School of Chemistry, University of Bristol, Bristol BS8 1TS, United Kingdom

²Department of Chemistry, University of Victoria

³Centre for Advanced Materials and Related Technology (CAMTEC), University of Victoria

⁴Department of Mechanical Engineering, Division of Medical Sciences, University of Victoria

⁵School of Biomedical Engineering, University of British Columbia

e-mail: imanners@uvic.ca

Nucleic acid (NA) therapeutics are now recognized as the third major medicine platform, alongside small molecules and biologics. In recent years, the promise of NA therapeutics has been indicated by successful treatments for diseases from COVID-19 to Cancer, yet key unsolved issues remain regarding the delivery of therapeutic NAs to target locations in vivo. Potential NA delivery vehicles face a host of challenges at organismal, tissue, and cellular levels.^[1]

Precision nanomedicine has emerged as a promising solution to overcome many of these barriers through modulation of every aspect of the nanomaterial's design: particle size, shape, dispersity, rigidity, surface chemistry, colloidal stability and more. Whilst preliminary studies have shown that particle shape affects the fundamental interaction of nanoparticles with the biological milieu, such studies are limited by the limited methods for producing non-spherical materials. When non-spherical nanomaterials are produced, control over particle dispersity is usually absent. 1D nanoparticles such as nanofibers have shown great promise over spherical nanoparticles, with reports of improved cell uptake, blood circulation, and tumor penetration and more.^[2]

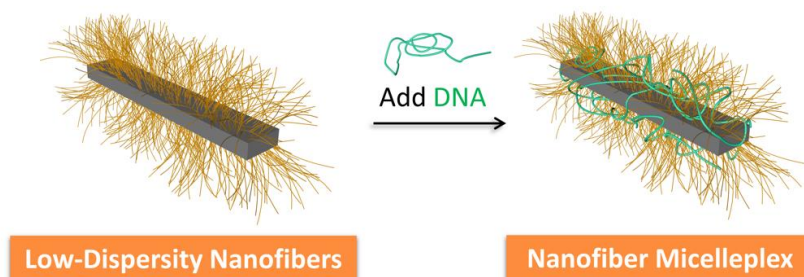


Figure 1. Formation of a precision polymer nanofiber micelleplex from a precision polymer nanofiber.

In this work we utilize living crystallization-driven self-assembly to produce precision polymer nanofibers^[3] that can complex NAs and successfully deliver them to cells.^[4] These particles are termed ‘nanofiber micelleplexes’ (Figure 1). We compare precision nanofiber micelleplexes of different lengths to nanosphere micelleplexes, revealing the important role that nanoparticle shape plays in nucleic acid delivery.^[3]

References

[1] W. Poon, W. C. W. Chan et. al. *Nat. Nanotechnol.* **2020**, *15*, 819–829.

[2] C. Kinnear, A. Petri-Fink et. al. *Chem. Rev.* **2017**, *117*, 11476–11521.

[3] S. T. G. Street, I. Manners et. al. *Polym. Chem.* **2022**, *13*, 3009–3025

[4] S. T. G. Street, S. M. Willerth, I. Manners et. al. *J. Am. Chem. Soc.* **2022**, *144*, 19799–19812.

This work was supported by the EPSRC (UK) (EP/N509619/1) and NSERC (Canada).

Fabrication capabilities at the UBC Nanofabrication Facility node of the Quantum Colab

**Andrey Blednov, Khush Hydri, Kostis Michelakis, Mario
Beaudoin, Matthias Kroug**

Advanced Nanofabrication Facility and Quantum Colab
Stewart Blusson Quantum Matter Institute
University of British Columbia
e-mail: beaudoin@physics.ubc.ca

In this poster, we will be presenting a brief overview of the micro- and nano-fabrication capabilities at the UBC Advanced Nanofabrication Facility (ANF). The ANF is part of one node of the Quantum Colaboratory (Q Colab). The Q Colab is a three-university partnership between Waterloo, Sherbrooke and British Columbia which aims to bring unique tools and knowledgeable staff across the Quantum Innovation Cycle.

Detection of SARS-CoV-2 by Localized Plasmon Resonance (LSPR)

Ariadne Tuckmantel Bido¹, Katie Amber², Frederic Leblond², A. G. Brolo^{1,3*}

¹University of Victoria, Department of Chemistry

²Centre Hospitalier de L'Université de Montréal Research Center (CRCHUM)

³Centre for Advanced Materials and Related Technologies

e-mail: agbrolo@uvic.ca

As of November 23, 2022, the severe acute respiratory syndrome coronavirus 2 (SARS-CoV-2) pandemic has reached 635.7 million confirmed cases with 6.6 million deaths worldwide.¹ This work addresses the need for a rapid, cheap, and easily scalable screening for SARS-CoV-2. A study paring nasopharyngeal swabs with saliva for SARS-CoV-2 patients concluded that saliva is similarly sensitive to nasopharyngeal swabs using molecular diagnosis (such as RT-PCR).² The Localized Surface Plasmon Resonance, or LSPR biosensing is based on the sensitivity of the plasmon frequency to local refractive index changes at the nanoparticle surface. The maximum of the extinction spectra of the sensor is assessed before and after the contact with the patient's saliva. If a redshift of the maxima is observed, the patient should be referred to further testing. If no significant change is observed the patient is healthy.

Figure 1 shows the result of plates tested on the Centre Hospitalier de L'Université de Montréal Research Center (CRCHUM). The sensors were able to differentiate the sick patients from the healthy ones (Fig 1B) and to detect antibody in the saliva of hospitalized patients (Fig 1A).

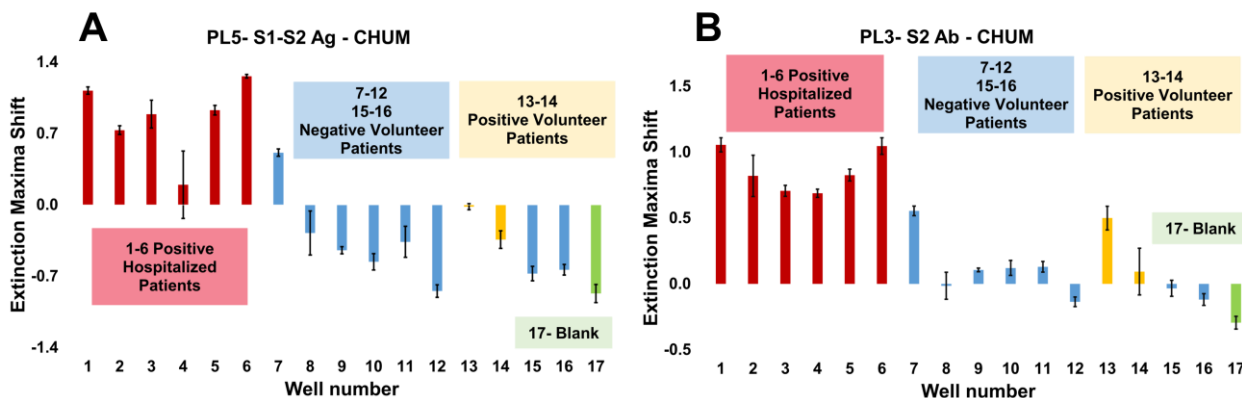


Fig. 1. Results of plates tested at CHUM for positive patients (hospitalized and not hospitalized) and negative patients for A) S1-S2 antigen on the plate and B) S2 antibody on the plate

This work was supported by NSERC and CFI (Canada Foundation for Innovation).

Acknowledgement

The authors acknowledge the scientific and technical assistance of the CAMTEC Facilities at University of Victoria, the partnership with CHUM and ImmunoPrecise Antibodies (IPA) for providing antibodies for tests.

References

- [1] who.int/health-topics/coronavirus, accessed 23/11/2022
- [2] Bastos, M. L.; Perlman-Arrow, S.; Menzies, D.; Campbell, J. R. *Ann Intern Med*, **174** (4), 501–510 (2021).

Halide Perovskites for Direct Conversion Megavoltage X-Ray Detector

S Kundu,¹ J O'Connell,² A Hart,² D Richtsmeier,² M Bazalova-Carter,² M I Saidaminov^{1,3*}

¹Department of Chemistry, University of Victoria

²Department of Physics and Astronomy, University of Victoria

³Centre for Advanced Materials and Related Technologies

e-mail: msaidaminov@uvic.ca

Megavoltage (MV) X-ray detectors used in cancer treatment either suffer from low sensitivity (scintillators) or prohibitively high cost (direct conversion). Here solution-processed direct-conversion MV X-ray detectors are demonstrated based on halide perovskites. The authors' prototype devices show a sensitivity of $\approx 0.7 \mu\text{C Gy}^{-1} \text{cm}^{-2}$, high photon-to-carrier conversion efficiency of 42 500%, and a signal-to-noise ratio of ≈ 1750 to 6 MV X-ray beam of a medical linear accelerator. The detector shows a contrast of over $\approx 1.5\%$ per cm of solid water, comparable to state-of-art commercial gadolinium oxysulfide (GOS) MV X-ray scintillators. This work demonstrates the first prototype of low-cost and efficient direct-conversion MV X-ray detectors.

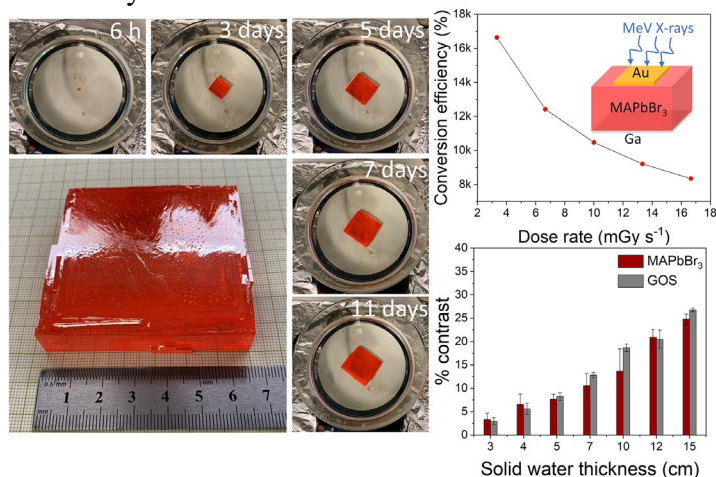


Fig 1. Large single crystal growth MAPbBr₃ for MV detector. Change of photon-to-carrier conversion efficiency with applied bias at 10 mGy s⁻¹ dose rate. Contrast with respect to thicknesses of solid water for medial imaging of MAPbBr₃ and commercial (GOS) detector.

This work was supported by New Frontiers in Research Fund—Exploration and University of Victoria Collaborative Health Grant. The authors thank BC Cancer (Provincial Health Services Authority in British Columbia, Canada) for providing the testing facility. The authors thank Jon Eby for developing an X-ray shutter system which enabled high frequency measurements.

Evaluation and Metrology of Surface-Enhanced Raman Scattering (SERS) substrates

Arash Azarakhshi,^{1,2} Li-Lin Tay³, Alexandre G. Brolo^{1,2,4}

¹ Department of Chemistry, University of Victoria, BC, Canada

² Department of Physics and Astronomy, University of Victoria, BC, Canada

³ Metrology Research Centre, National Research Council Canada, Ottawa, ON, Canada

⁴ Center for Advanced Materials and Related Technologies (CAMTEC), University of Victoria, BC, Canada
e-mail: agbrolo@uvic.ca

Surface-enhanced Raman scattering (SERS) is a large increase in the Raman response observed from molecules adsorbed on metallic nanostructures [1]. The possibility of generating vibrational (molecular fingerprinting) spectra from species at ultra-low concentrations is a characteristic of the SERS effect that has driven a large amount of potential applications in analytical and bioanalytical chemistry. However, despite important progress in the area in the last few decades, SERS is still not a widely applied standard analytical tool [2,3]. Issues of spectral variation and quantification are at the heart of the challenges to the implementation of SERS in analytical laboratories. These issues arise from the requirement for specific nanostructured metallic surfaces to support the effect, known as “SERS substrates”. There is a variety of SERS substrates fabricated from either top-down or bottom-up approaches. Each one of them presents a particular set of advantages and disadvantages. The understanding of the characteristics of a substrate is a very fundamental step in the field and it is, in principle, essential for the wide application of the technique. In general, the evaluation and comparison of SERS substrates are reported from a single parameter called the “enhancement factor” (EF). We suggest a set of parameters that can be used for substrate quantification [4], with the main goal of developing a set of standard measurements that can be used to evaluate a particular nanostructured surface used in SERS. We have considered two different types of molecular probes, Nile blue A and Pyridine, and implemented our procedures in two distinct commercially available SERS substrates. Thousands of SERS spectra (required for statistically significant analysis) were obtained for all systems in two extreme conditions, namely “average SERS” and “high fluctuation SERS” conditions. The average SERS implies solution concentrations in the millimolar regime, where the temporal fluctuations in SERS intensities were minimal. On the other hand, in high fluctuation SERS conditions, when the analyte concentrations reached nanomolar values, the SERS intensities present strong fluctuations that can be attributed to a small number of species visiting strongly localized plasmonic hotspots. Spatial and temporal histograms of the SERS intensities were obtained for all substrates and analytes at different concentrations and seven new evaluation parameters, related to hotspot strength, density, and uniformity were obtained. These new parameters provided a comprehensive space to compare the substrates and evaluate their efficacy beyond a single metric (EF).

References

- [1] Langer, J.; Jimenez de Aberasturi, D.; Aizpurua, J; et al., *ACS Nano*, (2019), **14**, 28.
- [2] Fan, M., Andrade, G. F. S.; Brolo, A. G. , *Analytica Chimica Acta*, (2020), **1097**, 1.
- [3] Bell, S. E. J, Charron, G.; Cortes, E; et al, *Angew Chem Int Ed Engl*. (2020), **59**, 5454.
- [4] Kiefl, E.J.; Kiefl, R. F.; dos Santos, D.P.; et al, *The Journal of Physical Chemistry C*, (2017), **121** (45), 25487.

“Determining effects of cementitious repair materials on embedded steel reinforcement exposed to chloride environment using electrochemical NDT”

P. Rodulfo¹

¹ University of Victoria, Department of Civil Engineering
e-mail: rodulfop@uvic.ca

Abstract

Electrochemical NDT techniques: Half-Cell Potential (HCP), Macrocell current (MC) and Linear Polarization Resistance (LPR) were used in this study to measure and monitor corrosion potential, current passed and the corrosion current rate on the three types of cementitious repair materials against that of a concrete substrate using Ordinary Portland Cement. The effectiveness of repair materials assessed in this study when monitoring the corrosion potential, current passed and corrosion current rate, when exposed to a chloride environment against that of a concrete substrate using Ordinary Portland Cement was determined. From the Electrochemical NDT results, it was found that Mix F outperformed Mix M and Mix P when exposed to a chloride environment.

Further examination of the three different repair cementitious materials was done through Scanning Electron Microscope (SEM) and Energy Dispersive X-ray (EDX) analysis. Through the EDX microscopy analysis, it was found that Mix F cementitious repair material was the one showing the least amount of chloride per % atomic weight of sample compared to Mixes P, M. As a result, Mix F was the most effective in delaying or retarding the transport of chloride ions reaching the rebar through the concrete matrix and initiating the corrosion process.

Furthermore, observation of all the repair materials through SEM showed that the Mix F repairs have the densest microstructure. The results obtained in this study helped in the determination of the best cementitious repair material for the inhibition of corrosion of RC structures in contact with marine environments.

3D Printing of Cardiac Tissues Derived from Human-Induced Pluripotent Stem Cells Using an Electroconductive Bioink

V. A. da Silva¹, M. R. Perez¹, S. Willerth^{1,2,*}

¹Department of Mechanical Engineering, University of Victoria

²Division of Medical Science, University of Victoria

e-mail: victor_alisson96@hotmail.com

Heart disease generates a huge burden on both the healthcare system as well as the economy. An emerging approach for studying heart disease uses 3D cardiac tissue bioprinting due to its potential to mimic cardiac tissues found in-vivo as a way to facilitate personalized drug screening. However, several parameters must be considered to achieve a functional tissue and for this end, this work aims to establish a novel bioink constituted of natural biomaterials (fibrin, alginate, gelatin) combined with a synthetic electroconductive biomaterial poly[3,4-ethylenedioxythiophene]: polystyrene sulfonate (PEDOT:PSS) for bioprinting cardiomyocytes (CM) derived from human induced pluripotent stem cell (hiPSCs). Preliminary results suggest successful differentiation of hiPSCs into CM through Wnt/ β -catenin signaling modulation, which spontaneously beats after 10 days of treatment (50 ± 2 bpm) and after 19 days expresses cardiac troponin T (cTnT), a tropomyosin-binding subunit of troponin complex that regulates muscle contraction. To ensure printability, we determined the optimal concentrations for the natural biomaterials as 1% (w/v) high-viscosity alginate, 7% (w/v) gelatin and 20 mg/mL fibrinogen. Further experiments will incorporate PEDOT:PSS to the bioink, as well analyze its mechanical and electrical properties. We will use this novel bioink to print CMs and characterize the functionality, viability, and cellular expression of the constructs. Thus, validating that the bioink developed through this project allows the creation of 3D models suitable for drug-screening studies.

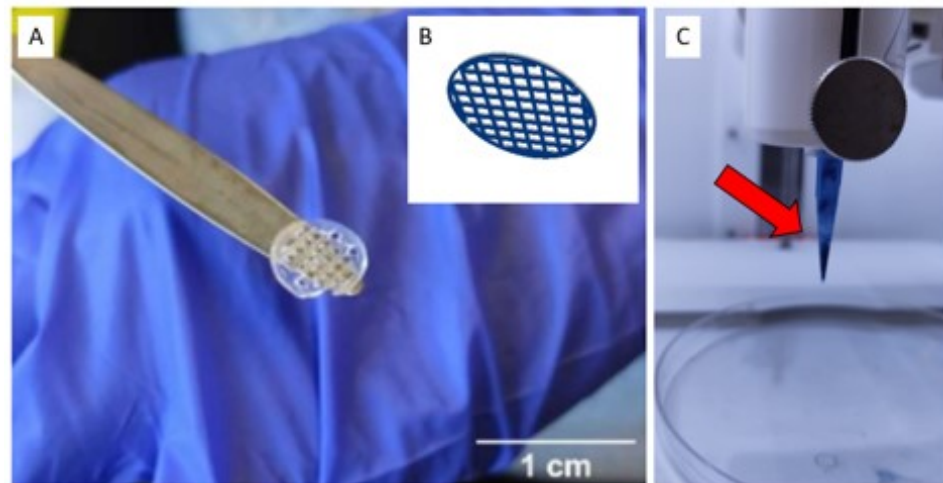


Fig.1. (A) Construct of Fibrin, alginate and gelatin without cells; (B) Three-dimensional design; (C) Clogged nozzle with bioink associated to PEDOT:PSS

This work was supported by NSERC, CRC program and MITACS

Investigating Spectrum of Double Nanoholes with Different Aperture and Gap Sizes

Behnam Khosravi¹, Reuven Gordon^{1,*}

¹Department of Electrical and Computer Engineering, University of Victoria, Victoria, BC, Canada
e-mail: rgordon@uvic.ca

Double nanoholes in metallic films can be used for trapping nano particles and single molecules in the gap between the holes. The resonance frequencies in the transmission spectrum depend on the size of the holes and the gap width in between. By tailoring these dimensions, the peaks can be shifted towards the desired frequency. These peaks are due to the wedge and gap plasmonic resonances in the structure [1].

The fabrication process involves colloidal nanolithography with polystyrene nanospheres and gold deposition on a glass surface, which forms double nano holes shown in Fig. 1A with a gap width of a few nanometers [2]. Nanospheres with different sizes and etching times were used to make holes with different gap widths.

By using FDTD simulations, enlarging the holes diameter redshifts the peaks for hole resonances. By changing the gap width, the gap resonance shifts correspondingly. Transmission spectrum of a double nanohole with hole diameter of 150 nm is shown in Fig. 1B.

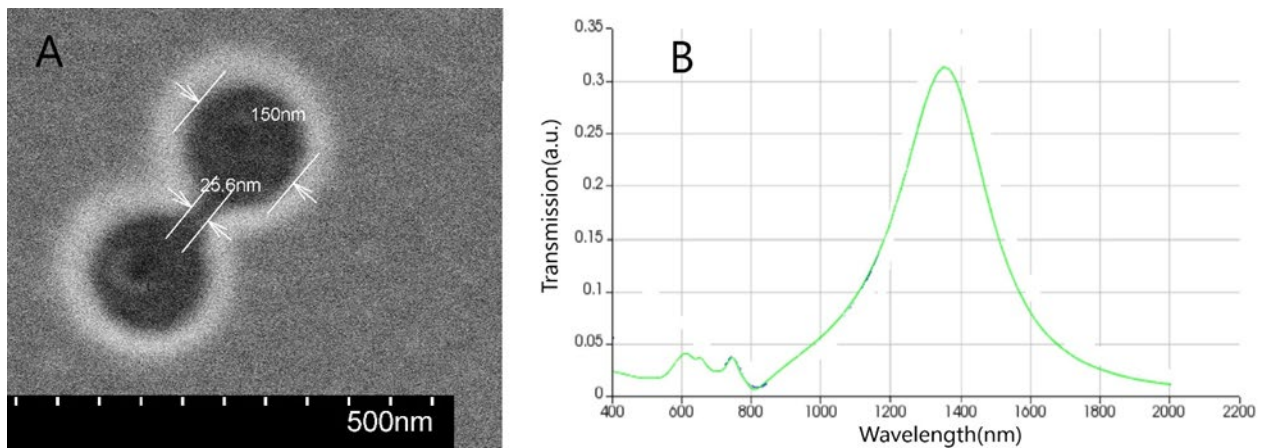


Fig. 1. A) SEM image of a double nanohole on a 70nm thick gold layer. B) FDTD simulation of transmission spectrum through a double nano hole of the same size as Fig. 1 (A).

The optical setup used for trapping nanoparticles, used a vertical sample placement and a novel cross-polarized-reflection geometry. The holes on the sample surface were visible using an infrared LED and a CMOS camera. The laser beam observed in the camera, comes from the reflection from the sample surface. This reflection-based method simplifies the alignment of microscope lenses and sample placement. A polarizing beam splitter have been used to observe the polarization change of the laser beam reflection from double nanoholes.

References

- [1] Chen Y, Kotnala, A, Yu L, Zhang J, Gordon R, 2015, Opt. Express, 23, 30227-30236.
- [2] Ravindranath AL, Shariatdoust MS, Mathew S, Gordon R, 2019, Opt. Express, 27, 16184-16194.

Post-fabrication trimming of silicon photonic cavities via localized surface oxidation

J. Fabian^{1,2}, D. Witt^{1,2}, K. Gardner¹, M. Mitchell¹, A. Pfenning¹, J.F. Young^{1,3}, L. Chrostowski^{1,2}

¹ Stewart Blusson Quantum Matter Institute, University of British Columbia

² Department of Electrical and Computer Engineering, University of British Columbia

³ Department of Physics and Astronomy, University of British Columbia

e-mail: jfabian@ece.ubc.ca

Optical resonators play a key role in many photonic quantum information technologies [1-3]. In silicon photonics, these cavities can be used to optically interface spin qubits, for which the resonance wavelength of the resonator has to be precisely matched with the optical transition frequency of the qubit [3]. Due to fabrication imperfections, a majority of the resonators must be corrected for their detuned resonance wavelength on the order of at least a few nm. In this work, we demonstrate laser-assisted local surface oxidation [4] of individual silicon photonic slot-bridge nanobeam cavities [5] as a permanent non-damaging post-fabrication trimming method.

Figure 1 (a) shows a pre-trimming SEM image of the studied slot-bridge nanobeam cavity, fabricated on a 220 nm silicon-on-insulator substrate. The cavity is based on a design proposal by Choi et al. [5]. The center of the cavity is formed by connecting the innermost holes with an 80 nm slot, spanned by a 45 nm central bridge. This configuration allows for extreme dielectric mode confinement with mode volumes down to $V = 0.004 \lambda_0^3$. Figure 1 (b) shows a SEM image of the same cavity post-trimming for which no structural degradation is visible. Figure 1 (c) shows the normalized transmission spectra pre- (red crosses) and post-trimming (blue dots). With the correct conditions of laser power, spot size and oxidation time, the cavity resonance permanently blue-shifts by $\Delta\lambda = 10$ nm while only slightly decreasing in its quality factor by 12% from 10200 to 8900. Figure 1(d) shows an image of a cavity used to establish the damage threshold for the process.

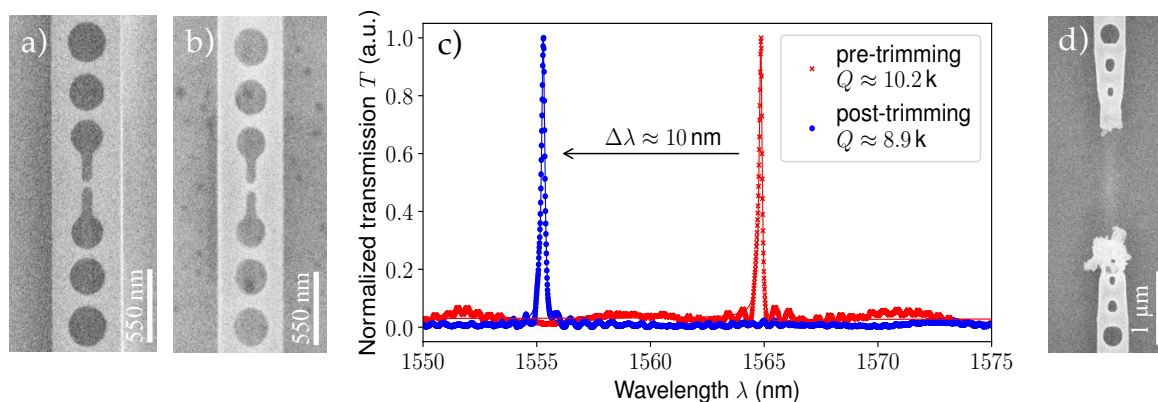


Fig. 1. (a) and (b) SEM images of the cavity pre- and post-trimming, respectively. No structural change is visible. **(c)** Normalized transmission spectra pre- (red crosses) and post-trimming (blue dots) with a peak shift of $\Delta\lambda = 10$ nm. **(d)** SEM image of a molten test cavity (different device than in (a) and (b)).

References

- [1] K. J. Morse et al., *Sci. Adv.*, vol. 3, no. 7, p. e1700930, Jul. 2017
- [2] X. Yan et al., *Adv Quantum Tech*, vol. 3, no. 11, p. 2000011, Nov. 2020
- [3] X. Yan et al., *APL Photonics*, vol. 6, no. 7, p. 070901, Jul. 2021
- [4] C. J. Chen et al., *Opt. Express*, vol. 19, no. 13, p. 12480, Jun. 2011
- [5] H. Choi, M. Heuck, and D. Englund, *Phys. Rev. Lett.*, vol. 118, no. 22, p. 223605, May 2017

Towards high throughput testing of low mechanical loss coating materials for gravitational wave detectors

K. Gardner¹, D. Wong^{1,2}, D. Bruns^{1,2}, M. Mitchell¹, Fengmiao Li¹, J. McIver², K. Zou^{1,2}, J. Rottler^{1,2}, J.F. Young^{1,2}

¹ Stewart Blusson Quantum Matter Institute, University of British Columbia

² Department of Physics and Astronomy, University of British Columbia

e-mail: kirsty.gardner@ubc.ca

The global network of ground-based gravitational wave detectors will undergo a suite of upgrades over the next decade to increase its sensitivity and astrophysical reach [1]. In the most sensitive frequency range of these detectors, the dominant noise source is thermal noise from the high reflectivity optical coatings on each detector's mirrors [2]. Testing of new low-mechanical loss (low noise) thin-film materials is therefore required to identify a next-generation coating material in advance of planned upgrades. There is a large parameter space of materials and deposition conditions to be explored, which would benefit from high-throughput testing to rapidly identify the best coating material. Current testing methods are not well suited to high-throughput testing as they use large substrates, onto which the thin film of interest is deposited, and measure these one-by-one [3].

We are developing an on-chip approach which uses mechanical microresonators (microdisks) as the devices onto which thin-film materials can be deposited and tested. By 'miniaturizing' the test devices in this way, we achieve ~ 100 devices per chip, and high throughput testing is easily achievable via either free-space optics or integrated waveguides. Here, we show progress towards development of this high-throughput testing method including fabricated devices, our free-space setup for characterizing the microdisks, and some first measurements of ringdowns in uncoated microdisks.

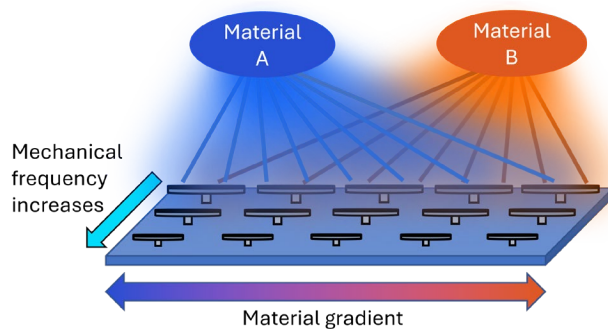


Fig 1. Schematic representation of our on-chip approach.

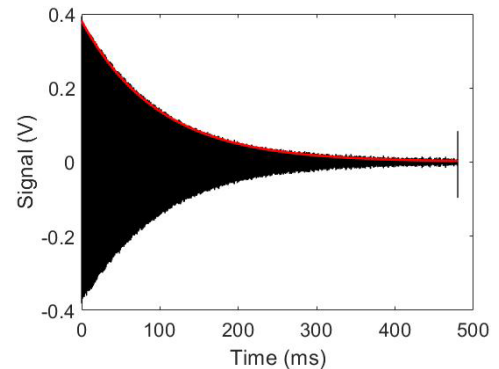


Fig 2. Ringdown data from an uncoated microdisk ($Q = 2.4 \times 10^4$).

We gratefully acknowledge financial support from the New Frontiers in Research Fund, the Stewart Blusson Quantum Matter Institute, and CMC Microsystems.

References

- [1] G. Vajente, L. Yang, A. Davenport, et al. *Phys Rev Lett.*, **127**, 071101 (2021).
- [2] T. Hong, H. Yang, E. K. Gustafson, R. X. Adhikari, and Y. Chen, *Phys. Rev. D*, **87**, 082001 (2013).
- [3] E. Cesarini, M. Lorenzini, and E. Campagna, *Rev. Sci. Instrum.*, **80**, 7 (2009).

Incorporating Insoluble Ionomers into the Catalyst Layers of Anion Exchange Membrane Fuel Cells - From Synthesis to Application

Matthew Siebert¹, Anastasiia Konovalova, Simon Cassegrain, Steven Holdcroft²

Department of Chemistry, Simon Fraser University, Burnaby BC, Canada

e-mail: ¹Matthew_Siebert@SFU.ca, ²Holdcrof@SFU.ca

Interactions between components of catalyst layers (CL) in fuel cells is an understudied area of research. Typically, components of a CL are a catalyst deposited on carbon and an ionically conductive polymer binder. Anode and cathode CL coated on either side of an ion exchange membrane creates the membrane electrode assembly (MEA). The pathway of the electrochemical reaction starts in the electrode's CL where dissolved gas reaches catalyst active sites, and the produced ion then passes through the membrane to the other electrode. Dissolving and incorporating ionomer as a binder is common practice, however, this leads to indirect ionic pathways, clogging of catalyst active sites and overall, to the increase in ion transport resistance across the MEA. Recent work on proton exchange membrane fuel cells has shown that the addition of insoluble ionomer particles can create pathways of low resistance for ions within the system. This work seeks to synthesize robust, insoluble anion exchange ionomer, incorporate it into CLs and explore the effects of these pathways within an anion exchange fuel cell.

References

- [1] Skalski T. J. G., Cassegrain S., Konovalova A., Fraser K., Holdcroft S. Synthesis of Caustic-Resistant Polymeric Ionic Liquids: Polyvinyl (C-2 Protected) Imidazoliums. Manuscript in preparation.
- [2] Hermán V, Takacs H, Duclairoir F, Renault O, Tortai JH, Viala B. Core double-shell cobalt/graphene/polystyrene magnetic nanocomposites synthesized by in situ sonochemical polymerization. RSC advances. **2015**;5(63):51371-81.
- [3] He C, Yang-Neyerlin AC, Pivovar B.S. Probing Anion Exchange Membrane Fuel Cell Cathodes by Varying Electrocatalysts and Electrode Processing. Journal of the Electrochemical Society. **2022**;169(2):24507.
- [4] Balogun E, Cassegrain S, Mardle P, Adamski M, Saatkamp T, Holdcroft S. Nonconformal Particles of Hyperbranched Sulfonated Phenylated Poly(phenylene) Ionomers as Proton-Conducting Pathways in Proton Exchange Membrane Fuel Cell Catalyst Layers. ACS energy letters. **2022**;7(6):2070-8.

Anion Exchange Membrane Water Electrolysis at Stainless Steel Electrodes

B. Chen, S. Holdcroft*

Simon Fraser University, Department of Chemistry

e-mail: holdcrof@sfu

Abstract

Anion exchange membrane water electrolysis (AEMWE) has great potential in hydrogen production, because it is efficient, low-cost and environmental-friendly. Increasing AEMWE works, showing high performance and long durability, have been reported recently. However, the study on gas diffusion layers (GDLs) is limited. As a critical part of membrane-electrode-assembly (MEA) in AEMWE, GDL is usually used to protect the catalyst layer, but GDL itself can also be a great catalyst. Here, AEMWEs with and without Ir black (anode catalyst) are studied. The results show that the stability of various GDLs follow a trend: high purity Ni felt > stainless steel (SS) felt >> NiCr alloy felt, while the SS felt shows a remarkable oxygen evolution reaction (OER) activity over other two. Although the SS felt is frequently used in AEMWE, its remarkable OER activity was not reported. Due to the coverage of anode catalyst layer (usually Ir based nanoparticles) between membrane and GDL, only a portion of OER occurs on the GDL and the performance is dominant by the catalyst layer (ionomer and catalyst). In this work, we reveal the significant role of GDL can play and hopefully provides the readers some insights to improve AEMWE performance and durability.

Development of a Carboxymethyl-chitosan/Alginate/Fibrin-based Bioink for Bioprinted Scaffold-mediated Gene Delivery

A. Juraski^{1,2*}, A. Azzoni¹, S. Willerth²

¹Azzoni Lab, Chemical Engineering, University of Sao Paulo, Sao Paulo, BRAZIL.

² Willerth Lab, Mechanical Engineering Department & Division of Medical Sciences, University of Victoria, Victoria, CANADA.

*e-mail: amanda.juraski@usp.br

Tissue lesions, such as spinal cord injury (SCI), are usually accompanied by changes in the tissue's physiological composition, gene expression, architecture, mechanical and physicochemical properties. Strategies that combine polymeric scaffolds for cellular support and organization with the delivery of endogenous molecules that can modulate the intra and extracellular environment present themselves as a promising route to overcome the limitations in current therapies. In particular, there is great interest in associating porous, anisotropic polymeric scaffolds with microRNAs. MicroRNAs inhibit messenger RNAs and therefore can prevent the translation of pro-inflammatory molecules, and scaffold-mediated gene delivery is a combinatorial approach for regenerating tissues with limited natural recovery, such as the spinal cord [1]. Carboxymethyl chitosan (CMChT), Alginate and Fibrin are interesting biomaterials for scaffolds due to their biocompatibility and chemical similarities to the extracellular matrix [2]. Considering the potential of combining tissue engineering and gene therapy, a CMChT/Alginate/Fibrin bioink was formulated to bioprint scaffolds combined with microRNAs associated with the regenerative process of SCI.

CMChT was synthesized in two different conditions, generating O-CMChT and N,O-CMChT. Different concentrations of CMChT and Alginate solutions (3%, 1.5% and 1% w/v) were prepared and combined with a 20 mg/mL solution of Fibrin. Samples were extrusion printed into a grid construct using a BioX Bioprinter (CELLINK) and printed into an Agarose bath. Following printing, scaffolds were crosslinked with a calcium chloride/thrombin solution for 10 min.

To generate constructs, we developed a printable bioink of 1.5% w/v CMChT, 1.5% w/v Alginate and 20 mg/mL Fibrin. Inks comprising lower (1.0% w/v) or higher (3% w/v) CMChT/Ag concentrations were associated with lower and higher viscosities, respectively, resulting in poorly defined scaffolds. Printability of the optimal bioink was supported by its uniform consistency, with minimal fluctuations in extrusion force (around 5 KPa) required for printing and indicative of homogeneity within the solution.

These findings indicate that a CMChT/Alginate/Fibrin bioprinted scaffold can be further explored for regenerative medicine therapies, such as tissue engineering and gene delivery. Next steps will include the printing with neuroprogenitor stem cells and microRNAs incorporated in the bioink.

This work was supported by grant No 88887.694651/2022-00 offered by the Brazilian Coordination for the Improvement of Higher Education Personnel.

References

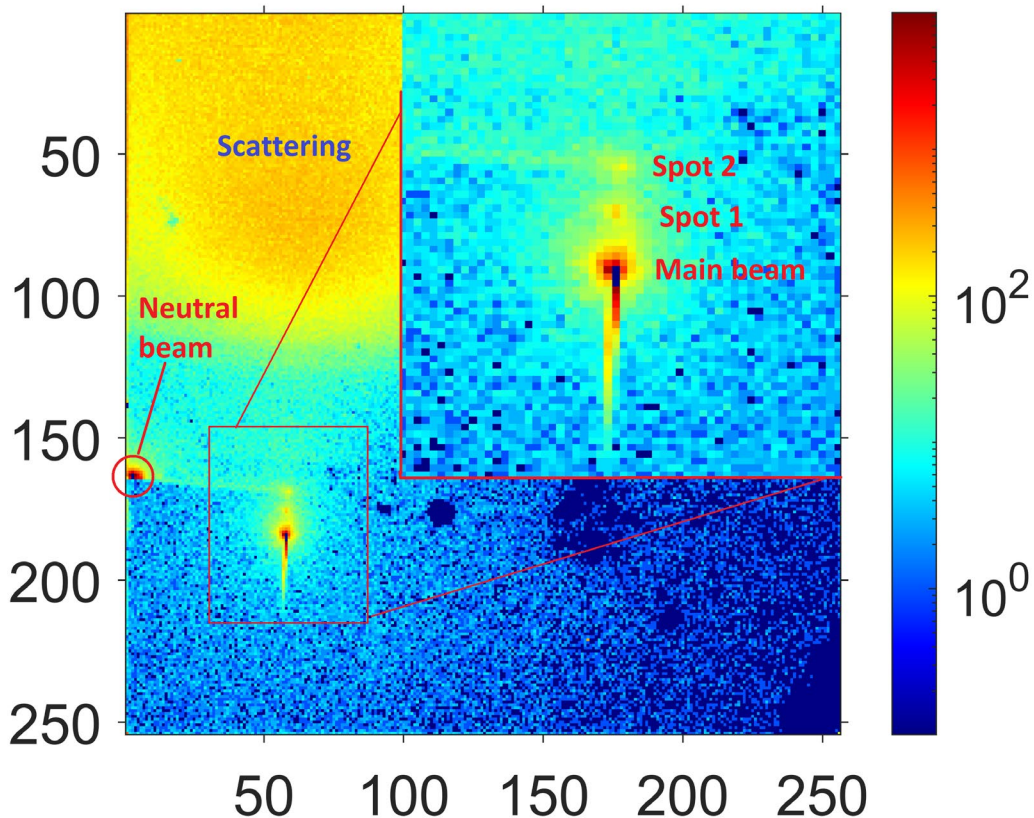
- [1] U. Milbreta, J. Lin, C. Pinese, *et al.* Scaffold-mediated sustained, non-viral delivery of miR-219/miR-338 promotes CNS remyelination. *Molecular Therapy*, v. **27**, p. 411–423, 2019.
- [2] L. Wang, L. Sun, Z. Gu, *et al.* N-carboxymethyl chitosan/sodium alginate composite hydrogel loading plasmid DNA as a promising gene activated matrix for in-situ burn wound treatment. *Bioactive Materials*, v. 15, p. 330-342. 2022.

Spots observed from glancing incidence He ion scattering from graphite

A. Bunevich, D. Lopez Silva, and K. L. Kavanagh,
Simon Fraser University, Burnaby, BC V5A 1S6 Canada
abunevic@sfu.ca

Our group is using a commercial Si complementary metal-oxide-semiconductor (CMOS) camera (Advacam, Minipix, 55-micron pixel pitch) to image scattering of a focused He⁺ ion beam (10 – 30) keV transmitted through various materials [1, 2]. The detection is via ion-generated electron-hole pair current in the array of surface barrier diodes in this camera [3]. We are trying to measure the spatial and temporal coherence length of the source by searching for evidence of interference. In this presentation, we will describe results from experiments involving glancing incidence scattering of our He⁺ ion beam from surfaces of highly-oriented pyrolytic graphite (HOPG) as a function of beam energy and sample tilt angle. Considering our camera pixel pitch and scattering geometry, we expect to be able to resolve diffraction peaks due to the smaller in-plane graphite, effective period. The figure attached shows an example of one result that will be discussed. *Acknowledgements: NSERC, SFU 4DLabs, CFI/BCKDF.*

- [1] Karen L. Kavanagh, Aleksei Bunevich, and Mallikarjuna Rao Motapothula, ArXiv submit/311553 [cond-matt.mes-hall] 3Apr 2020.
- [2] Jiaming Wang, Symphony H. Y. Huang, Christoph Herrmann, Shelley A. Scott, François Schiettekatte, and Karen L. Kavanagh. *J. Vac. Sci. Technol B* **36**, 021203 (2018); doi: 10.1116/1.5020667.
- [3] K. L. Kavanagh, C. Herrmann, J. A. Notte, *J. Vac. Sci. Technol. B* **35**, 06G902 (2017).



Creation of wide stopbands by loading split-ring-resonators to a terahertz guided-wave coplanar strip transmission line

Saeid Asadi¹, Levi Smith,¹ Thomas Darcie¹

¹ Department of Electrical and Computer Engineering, University of Victoria, BC, V8W, Canada

saeid.asadi86@gmail.com, levismith@uvic.ca, tdarcie@ece.uvic.ca

In this paper, split-ring-resonator (SRR) meta-atoms are placed between two coplanar strip (CPS) THz transmission line (TL), designed on a $1\mu\text{m}$ Si_3N_4 membrane enabling operation up-to 3 THz. Adding a SRR in a TL introduces a resonance corresponding to a negative permeability ($\mu < 0$) [1] which appears as a stopband [2]. In [3], equal sized meta-atoms are placed near a CPS TL leading to a single resonance and narrow stopband. In this work, we widen the stopband by varying the radius of each meta-atom. This study has been performed by Simulation (HFSS) and the ABCD matrix approach [4]. Fig. 1(a) illustrates a CPS TL loaded with a single SRR. In Figs. 1(b, c), the electric field intensity is observed off and on resonance, respectively. In Fig. 2, the TL containing one SRR is compared with TL containing three and four SRRs in terms of the S_{21} parameter. In Fig. 2(a), all the SRRs have the same radius. The TL with three SRRs has a wider stopband. In Fig. 2 (b), the radii of SRRs, of the TL with three SRRs, are changed which corresponds to a wide stopband and the region where $\mu < 0$. Also, we can further weaken components in the stopband as depicted in Fig. 2 (c).

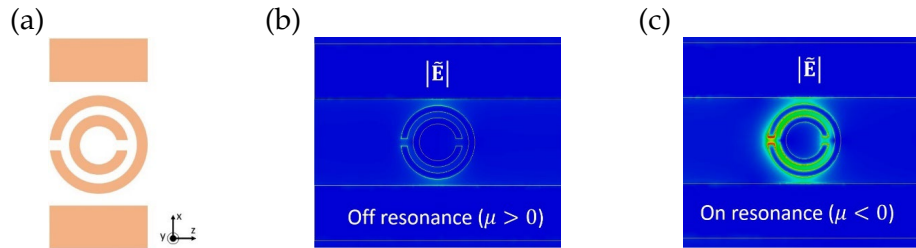


Fig. 1. (a) CPS TL containing a single SRR. (b) and (c) Electric field pattern in off and on resonance, respectively.

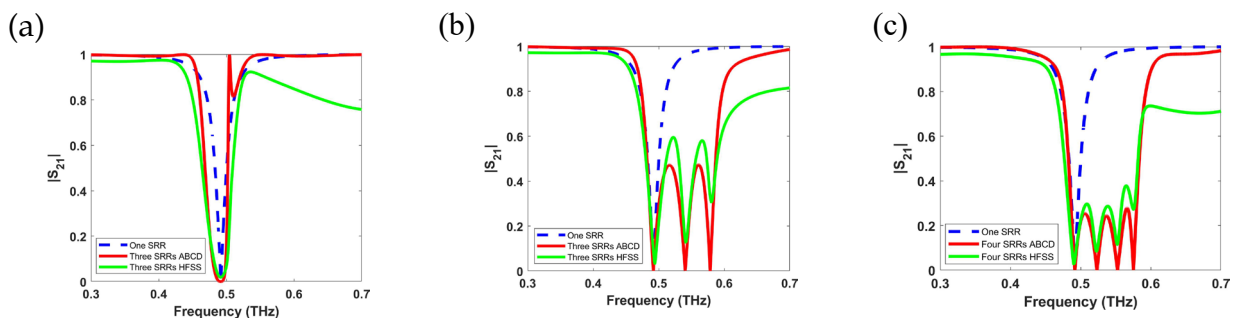


Fig. 2. S_{21} parameter of CPS TL containing SRRs. (a) SRRs have equal radii. (b) and (c) three and four SRRs with different radii, respectively

References

- [1] Pendry, J, B. Holden, A, J. Robbins, D, J. Stewart, W, J. 1999. *IEEE Transactions on Microwave Theory and Techniques*, **47**, 2075-2084.
- [2] Syms, R, R. A. Shamonina, E. Kalinin, V. Solymar, L. 2005. *J. Appl. Phys*, **97**, 064909.
- [3] Smith, L. Shiran, V. Gomaa, W. Darcie, T. 2021. *Optics Express*, **29**, 15-19.
- [4] Pozar, D, M. *Microwave Network Analysis, Microwave Engineering*. 2012, John Wiley & Sons, Inc, United States, 188-194.

Contact angle analysis of nanocoated self-cleaning surfaces for commercial application

L. Sharma¹, P. Raizada¹, M. Garg¹, R. Gupta^{1*}

¹Department of Civil Engineering, University of Victoria, Victoria, British Columbia, Canada
e-mail: guptar@uvic.ca

Pathogenic contamination of the surfaces has been proven to be a potent mode of transmission of contagious diseases. The transmissibility of the contagious pathogens on the high contact surface can be greatly reduced by modifying such surfaces to self-cleaning surfaces. The self-cleaning coating considers two aspects: (a) manipulating the chemical composition of the coating film to resist pathogens proliferation, (b) making surface hydrophobic that pathogens are less likely to adhere to surface. One of the key challenges is to ensure the commercial viability in terms of robustness, durability and aesthetics consideration while imparting the self-sanitizing properties into the coating. In this research, we have attempted to prepare the commercially viable nanocoating by modifying the commercial coating by introduction of the SiO₂, CuO, ZnO and TiO₂ nanofillers, due to their contribution towards providing protection against UV and bacteria. The contact angle was tested by using the Rame' Hart Tensiometer to measure the surface wettability of the sessile droplet. Additionally, the robustness of coating on each substrate was tested using adhesion pull-off testing. Thus, the modified coating has the potential application in coating to washing basins and counter tops to create a safe milieu.

Electrically Tunable Piezoelectric Vibration Energy Harvester (PVEH)

Sreekumari Raghavan, Rishi Gupta, Loveleen Sharma

Department of Civil Engineering,

University of Victoria.

e-mail: guptar@uvic.ca

Advancement in Structural Health Monitoring in real time mode has been enabled by the innovations in electronics and related technologies such as Micro Electro Mechanical Systems (MEMS). The journey to "Trillion Sensor World", where every critical structure can be monitored remotely, demands sustainable autonomous power sources for the sensor nodes. This has led to the focus on research towards realizing methods to convert the ambient energy that is already present in various forms, to usable electrical power. One of the sources is vibrations that is present in many structures and systems. The technology of vibration energy harvesting using piezoelectric materials is mainly based on the cantilever configuration. However, this configuration leads to a high output power at the resonant frequency and a sharp drop in output at frequencies before and after the resonant frequency.

This research focusses on a novel method to shift the resonant frequency of the harvester electrically to the varying ambient frequency. The design of the device incorporates another smart material viz., Ionic Polymer Metal Composites (IPMC) with the PVEH in the cantilever configuration. IPMC is a Nano-composite whose properties can be tailored during fabrication. It can work as an actuator when a low voltage in the range of 1 to 4 V is applied to it. The IPMC integrated above the cantilever beam of the harvester functions as a stopper and the contact with the beam changes the resonant frequency of the harvester. The cantilever beam has a thinner extension beam in order to provide a sensitive impact point for the low range force generated by the IPMC.

This work is on the experimental characterization and the theoretical analysis of the novel design. Macro Fiber Composite is used as the piezoelectric material and Nafion based IPMC is used for actuation. The results based on the various experiments indicate that the device can be tuned by applying a low voltage in the range of 1 to 4 V to the IPMC. This enables the generation of power from the harvester at frequencies other than the basic resonant frequency of the harvester.

It is observed that the shift in the resonant frequency of the harvester is proportional to the blocking force of the IPMC actuator. The blocking force is defined as the force that can be applied by the actuator with zero deflection. The parameters that decide the blocking force of IPMC are the input voltage, the cation concentration, the electrode configuration and the back bone material. For a given IPMC, the above mentioned parameters except the input voltage are constant. Hence, the control of the actuation property of IPMC is achieved by changing the input voltage to the IPMC. Experiments were carried out to study the performance of the harvester at different ambient frequencies, at different points of contact, at different gaps between the beam and the IPMC and at different acceleration conditions. Since the power required for the IPMC is low, it can be provided from the harvested power itself. The results indicate that the characteristics of the device is consistent.

Investigation of InGaN/GaN NW p-n junctions using Transmission electron microscopy.

Anitha Jose¹, Maria Tchernycheva², Cristina Cordoba³, Arthur Blackburn³, Martha McCartney⁴, and Karen L. Kavanagh¹

¹Department of Physics, Simon Fraser University, Burnaby, British Columbia, Canada

²Centre for Nanoscience and Nanotechnology - C2N (CNRS / Université Paris-Sud), 91120 Palaiseau, France

³Department of Physics and Astronomy, University of Victoria, Victoria, BC, Canada

⁴Department of Physics, Arizona State University, Tempe, AZ 85287, USA
e-mail: anithaj@sfu.ca

GaN based nanowires (NWs) have been applied in devices including light emitting diodes (LEDs) [1], photodetectors [2] and laser diodes [3]. We report the TEM characterization of an n-GaN/InGaN/p-GaN structure for potential applications as LEDs. The NWs were grown by Molecular Beam Epitaxy using Si and Mg as the n-type and p-type dopant, respectively, on a Si substrate. SEM images of the sample on the substrate showed two kinds of wires distinguishable by their lengths. One set were more than a micron long and the other about 700-800 nm. They differed also in the effects of In on TEM image contrast, rate of tapering of the diameters, and therefore, the expected junction positions. The longer wires had a sharp change in diameter on transitioning to the InGaN region whereas the shorter wires were of uniform diameter at the junction and tapered towards the bottom end of the wire. The longer n-type side on the top in the long wires had a high density of stacking faults when compared to the shorter wires. More experiments are underway to investigate both wires to compare the built-in voltage using electron holography [4].

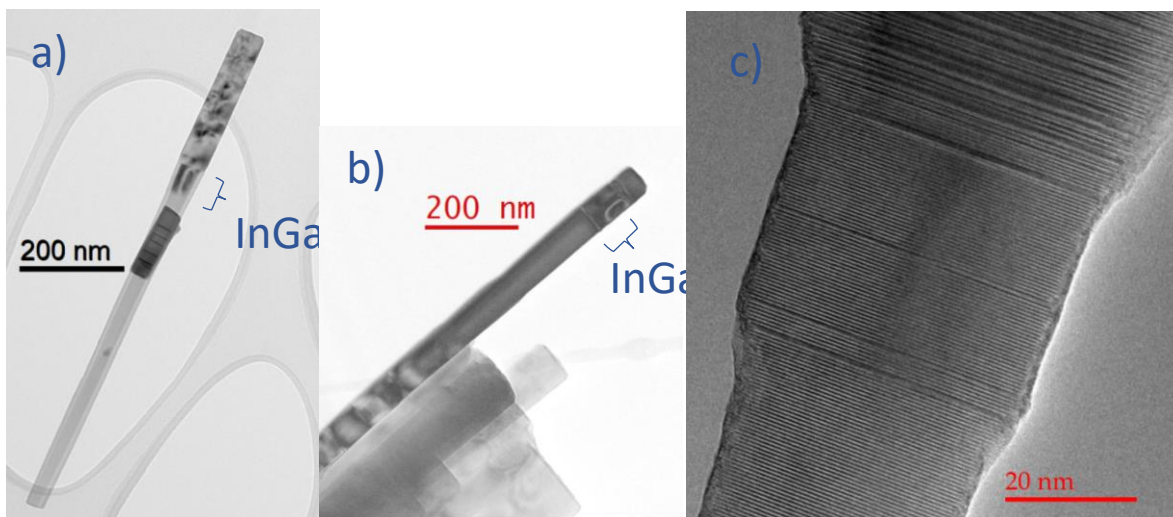


Fig 1. BF images of a) long and b) short wire. c) High-res image of the junction region in the long wire

Acknowledgement: NSERC.

References

- [1] C.-Y. Chen et. al, *ACS Nano*, **6**, 5687-5692 (2012).
- [2] X. Zhang et al, *J. Mater. Chem. C* **5**, 4319-4326 (2017).
- [3] J. Heo et al, *Appl.Phys. Lett.* **98**, 21110 (2011).
- [4] M. Lehmann and H. Lichte, *Microscopy and Microanalysis* **8**, 447 (2002).

Surface Enhanced Raman Spectroscopy for Community-based Drug Checking

R. Martens¹, L. Gozdziński¹, B. Wallace^{2,3}, D. Hore^{1,4}

¹Department of Chemistry, University of Victoria

²School of Social Work, University of Victoria

³Canadian Centre for Substance Use Research

⁴Department of Computer Science, University of Victoria

The ongoing overdose crisis has furthered the need for community-based drug checking services as well as inspiring the development of new drug checking methods for rapid detection of opioid mixtures. Given the fluidity and constant evolution of the current drug supply, the detection of benzodiazepines has been of particular interest for drug checking. With growing numbers of overdose deaths having detected benzodiazepines within the drug mixture, it prompts further research into drug characterization of these adulterants. A particular drug of interest with similar effects to benzodiazepines has been xylazine. It's typically used as a sedative in veterinary practices and is now being used as a cutting agent in opioid samples. No research has been performed using human test subjects, so its full effect is unknown and thus its rapid emergence poses a serious hazard to the safety of people who use drugs. Developing new methods for the rapid detection and identity of benzodiazepines and sedatives in the current drug supply could act as a preventative measure for complicated overdoses. This work focuses on the exploration of surface enhanced Raman spectroscopy and its capabilities in detection, identification, and quantification of different adulterants in opioid mixtures. We will evaluate and compare two different experimental configurations. The first is based on 830 nm excitation, with the SERS substrates being 50 nm colloidal gold particles in solution[1]. The second setup uses 785 nm excitation with silver-based SERS substrates fixed onto solid supports.

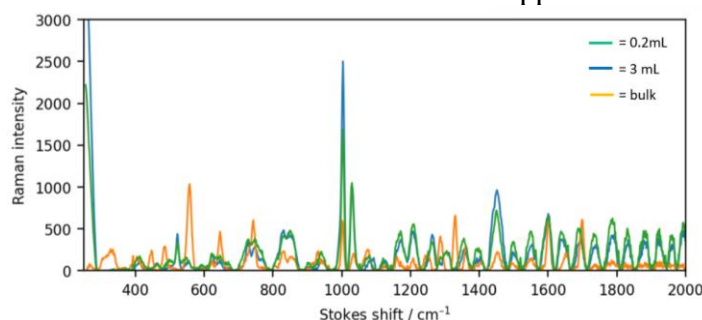


Fig. 1. SERS Spectra of 3.34% Xylazine sample in 0.2mL methanol and 3.0mL methanol, using silver-based substrate chips, and powdered Raman bulk scan. 10 measurements of each sample scan, averaged and overlaid

This work was supported by Agilent Technologies, BC Ministries of Mental Health and Addictions, Island Health, SpectraPlasmonics, and the Vancouver Island Drug Checking Project.

References

- [1] L. Gozdziński, A. Rowley, S. A. Borden, A. Saatchi, C. G. Gill, B. Wallace, and D. K. Hore, A. "Rapid and Accurate Etizolam Detection Using Surface-Enhanced Raman Spectroscopy for Community Drug Checking." *The International journal of drug policy*, 102, 103611–103611 (2022).

Accessibility of Guests to the Microenvironments of a Supramolecular Hydrogel Depends on the Guest's Structure

Ankur A. Awasthi^{1,2} and Cornelia Bohne^{1,2*}

¹ Department of Chemistry, University of Victoria, PO Box 3065, Victoria, BC, V8W 3V6, Canada.

² Centre for Advanced Materials and Related Technology (CAMTEC), University of Victoria, 3800 Finnerty Rd, Victoria, BC, V8P 5C2, Canada
e-mail: ankurawasthi@uvic.ca

Our objective is to determine the number and properties of microenvironments accessible to hydrophobic guests in sodium deoxycholate (NaDC) hydrogels. NaDC molecules self-associate into hierarchical structures that provide multiple binding environments to small molecules. Pyrene was used as a polarity sensitive probe to investigate this hydrogel. The ratio between the I and III peaks (I/III) in the pyrene monomer emission spectra reveals the polarity of the microenvironment around this probe.^[1] Steady-state and time-resolved fluorescence experiments were used to determine the accessibility of iodide (I⁻) and nitromethane (CH₃NO₂) quenchers to excited pyrene bound to the various sites of the gel. Pyrene is quenched more efficiently in the hydrophilic sites of the gel, as pyrene's I/III ratio decreases with increasing quencher concentration. Time-resolved data revealed three different lifetimes for pyrene molecules located in different sites of the NaDC hydrogel. The shortest lifetime was assigned to pyrene localized in the aqueous region of the gel, where excited pyrene is quenched most efficiently. The longest lifetime was assigned to pyrene in gel aggregates, with hindered or no access to I⁻ but access to CH₃NO₂. Pyrene with the intermediate excited state lifetime was assigned to a third location in the gel as it was quenched with a lower efficiency than for pyrene in the entrapped aqueous phase. Our results show that the NaDC hydrogel is comprised of at least three microenvironments to accommodate guests and each microenvironment has varying accessibility depending on the nature of the quencher. These results have relevance when incorporating hydrophobic drugs in gels, because the presence of various environments and the degree of access to these environments may influence the release kinetics of a drug from the gel.

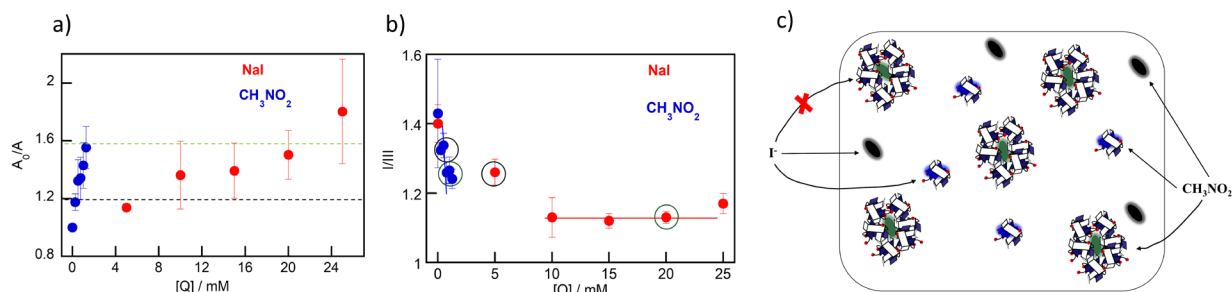


Fig. 1. a) Relative quenching efficiencies of I⁻ and CH₃NO₂ for excited pyrene in NaDC hydrogels. (b) Comparison of the I/III ratios for pyrene quenched in NaDC hydrogels by I⁻ and CH₃NO₂. Colored circles correspond to the A_0/A values shown with similar colored lines in Fig 1a. (c) Schematic representation of accessibility of each quencher to pyrene localized in different microenvironments of NaDC hydrogels.

References

[1] K. Kalyanasundaram & J. K. Thomas, *J. Am. Chem. Soc.* **99**, 2039–2044 (1977).

Influence of Materials and Device Parameters on Open-circuit Voltage of Organic Photovoltaics

J. M. Jailani¹, B. Nasrollahi¹, V. Pecunia^{1*}

¹Pecunia Research Group Sustainable Optoelectronics
School of Sustainable Energy Engineering, Simon Fraser University
e-mail: vincenzo_pecunia@sfu.ca

Organic photovoltaics (OPVs) have emerged as a promising alternative to conventional silicon (Si) photovoltaics for clean energy production due to their more favorable sustainability profile and their versatility for both indoor and outdoor energy harvesting. Moreover, OPVs present the advantage of being flexible, thin, and lightweight [1]. Although OPVs are promising, their power conversion efficiency (PCE) still lags behind Si photovoltaics. One of the key parameters that dictate the PCE of OPVs is the open-circuit voltage (V_{oc}), which represents the maximum voltage a solar cell can provide to an external circuit [2]. OPVs developed thus far barely exceed a V_{oc} of 1.0 V, which constitutes an important limitation. To overcome this challenge, it is critical to understand the origin of the V_{oc} in OPVs and the factors influencing it. In this poster, we show the origin of the V_{oc} in OPVs and present certain crucial device parameters such as the energy bandgap, work function, recombination, and charge transfer states of the donor and acceptor materials that majorly influence the V_{oc} [2,3]. In addition, suitable engineering of the donor-to-acceptor interface area to achieve an enhanced V_{oc} is discussed [4]. Moreover, the impact of varying light intensities on the V_{oc} of indoor OPVs is presented [5]. These insights highlight the device and materials parameters affecting the V_{oc} of OPVs, thereby providing the foundation for further advances in their efficiencies.

References

- [1] M. Benganem and A. Almohammed, *Advanced Structured Materials*, Springer Cham (2022)
- [2] N.K. Elumalai and A. Uddin, *Energy & Environmental Science*, **9**, 391-410 (2016)
- [3] C. Deibel et al, *Advanced Materials*, **22**, 4097-4111 (2010)
- [4] K. Vandewal et al, *Advanced Materials*, **26(23)**, 3839-3843 (2014)
- [5] M. Jahandar et al, *ChemSusChem*, **14(17)**, 3449-3474 (2021)

The complexity of the binding dynamics of aminonaphthalenes to cucurbit[7]uril

G. Lopes Camelo^{1,2}, C. Bohne^{1,2}

¹Centre for Advanced Materials and Related Technologies

²University of Victoria, Department of Chemistry

e-mail: gustavocamelo@uvic.ca

Cucurbit[*n*]urils, CB[*n*]s are barrel-shaped macrocycles with variable cavity sizes that allow tuning their affinity to hydrophobic guests and carbonyl-lined portals that can stabilize cationic charges, such as protonated naphthylammoniums^[1]. I have proposed a CB[*n*]-based host-guest assembly design in which the evolution of the system into a thermodynamic product can be diverted to a different outcome temporarily or indefinitely. I have focused on studying the separate binding epitopes of a ditopic guest molecule, initially, naphthylamines to CB[7].^[2,3]

Quantitative fluorescence measurements are enabled by a host-delayed proton transfer in the excited state of the guest. I am using stopped-flow fluorescence to determine the effect of structural modifications of the guest molecule on the dynamics for guest formation. The addition of methyl group substitution on the amino group of 2-aminonaphthalenes accelerated the association and dissociation dynamics but also favoured the formation of higher-order complexes with sodium cations, used as a concentration modulator of free CB[7].

The study of the dynamics of separate binding motives will aid the design of more sophisticated supramolecular architectures in complex mixtures. Creating ditopic structures that preserve high-fidelity of the binding parameters to the original guest will be the first step in establishing a parameter space in which kinetic control over supramolecular structures can be achieved.

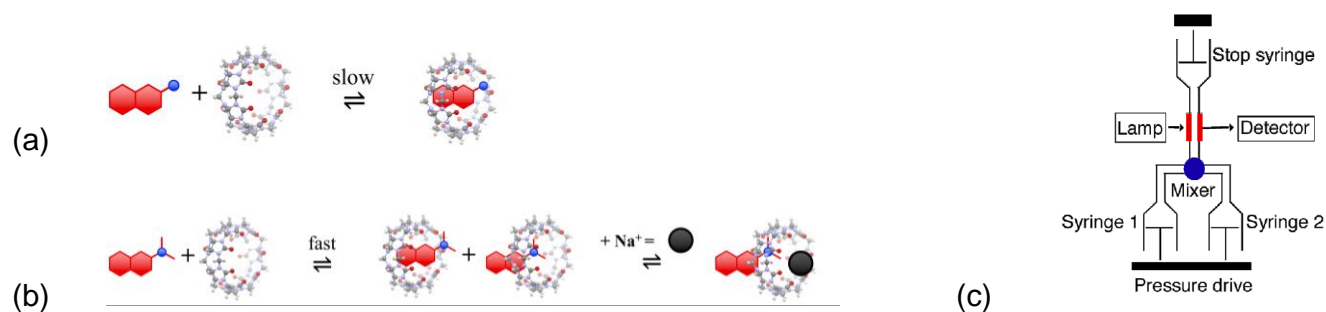


Fig 1. Kinetic scheme of (a) 2-aminonaphthalene cation (ANp⁺) and of (b) N-dimethyl-2-aminonaphthalene cation (DMANp⁺) binding to CB[7] with the formation of higher-order complexes with sodium. (c) Stopped-flow fluorescence setup^[4].

This work was supported by Natural Sciences and Engineering Research Council of Canada (NSERC)

References

- [1] J. W. Lee, S. Samal, N. Selvapalam, H.-J. Kim, K. Kim, *Acc. Chem. Res.* 2003, 36, 621-630.
- [2] S. S. Thomas, H. Tang, C. Bohne, *J. Am. Chem. Soc.* 2019, 141, 9645-9654.
- [3] K. Vos. PhD dissertation, University of Victoria, 2019, Victoria, BC.
- [4] C. Bohne, *Supramolecular Photochemistry* (Eds. V. Ramamurthy and Y. Inoue), JWS, Singapore, 2011, 1-51.

THz Band-stop Integrated Filter on a Thin Membrane

S. Dehghanian¹, L. Smith¹, T. Darcie^{1,*}

¹University of Victoria, Department of Electrical and Computer Engineering
e-mail: adehghanian@uvic.ca

The terahertz region of electromagnetic spectrum has become a significant research area due to its various applications in science. Effective terahertz wave filtering in systems requires integrated THz System-On-Chip (TSoC) components. A low-loss, low-distortion and low-pulse-dispersion TSoC has been demonstrated using Photoconductive Switch (PCS) devices bonded directly to a Coplanar Strip-line (CPS) transmission line defined using photolithography on 1 μ m-thin Si₃N₄ membrane [1]. Based on this capability, it is now possible to develop different components for the TSoC. Here, a novel THz band-stop filter integrated into the CPS transmission line is presented to reject specific spectral components.

Previous studies have demonstrated the operation of band-stop filters in the THz frequency range, working at a center frequency of 600 GHz. To characterize these filters, they were embedded in a micro-strip line attached to photoconductive switches that serve as THz emitters and detectors [2]. Some studies have also been conducted to filter THz specific spectrum using other materials such as graphene or silicon [3,4]. This work focuses on developing integrated, compact, and efficient TSoC technologies in which guided-wave THz systems replace the current free-space THz systems.

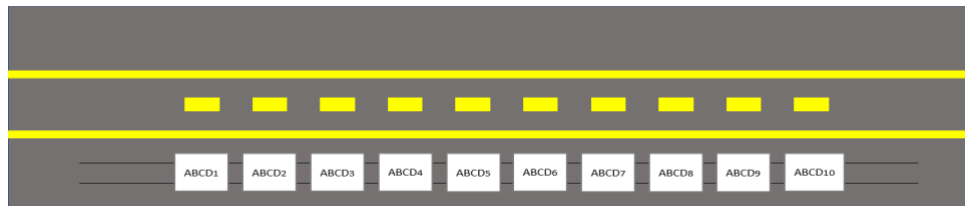


Fig. 1. Structure of band-stop filter integrated in CPS transmission line.

Here we analyze a structure compatible with experimental fabrication. We set N to be 10, and 20 to represent of longer filters. Fig.1 illustrates the complete structure and unit cells. The system was modelled using a cascade of two-port ABCD transmission matrices for lossy transmission lines. The cascaded ABCD matrices were then converted to S-parameters using standard methods (Fig. 2).

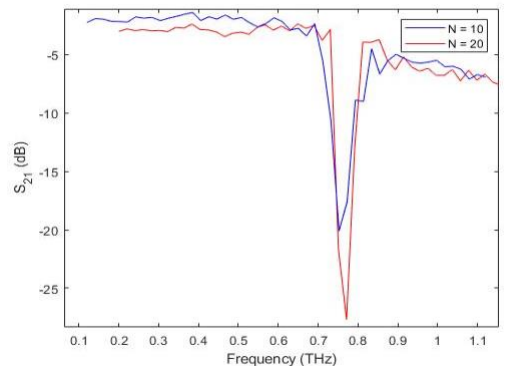


Fig. 2. Transmission Coefficient for N equal 10 and 20.

References

- [1] Smith, R., & Darcie, T. Demonstration of a low-distortion terahertz system-on-chip using a CPS waveguide on a thin membrane substrate. *Optics Express*, 27(2019)
- [2] Cunningham, J., Wood, C., Davies, A. G., Hunter, I., Linfield, E. H., & Beere, H. E. Terahertz frequency range band-stop filters. AIP Publishing (2022)
- [3] Ram, G. C., Sambaiah, P., Yuvaraj, S., & Kartikeyan, M. V. *Tunable bandstop filter using graphene in terahertz frequency band*. AEU - International Journal of Electronics and Communications. Retrieved February 11, (2022)

Repurposing Pyronaridine as a DNA Repair Inhibitor to Exploit the Full Potential of Gold Nanoparticle Enhanced Radiation Response

Nolan Jackson¹, Abdulaziz Alhussan¹, Kyle Bromma¹, Wayne Beckham^{1,2}, David Jay³, James C. Donnelly⁴, Frederick G. West^{3,4}, Afsaneh Lavasanifar⁵, Michael Weinfeld³ and Devika B. Chithrani^{1,6,7,8,9*}

¹ Department of Physics and Astronomy, University of Victoria

² British Columbia Cancer-Victoria

³ Department of Oncology, Division of Experimental Oncology, Faculty of Medicine & Dentistry, University of Alberta

⁴ Department of Chemistry, University of Alberta

⁵ Faculty of Pharmacy and Pharmaceutical Sciences, University of Alberta

⁶ Centre for Advanced Materials and Related Technologies, Department of Chemistry, University of Victoria

⁷ Centre for Biomedical Research, Department of Biology, University of Victoria

⁸ Division of Medical Sciences, University of Victoria

⁹ Department of Computer Science, Mathematics, Physics and Statistics, Okanagan Campus, University of British Columbia

e-mail: devikac@uvic.ca

The efficacy of current radiotherapy (RT) techniques is limited due to the normal tissue toxicity that is induced during treatment. For this reason, the ability to increase radiosensitization in tumors is essential to improve curative results. Gold nanoparticles (GNPs) exhibit radiosensitizing properties through an increase in DNA damage, and by complementing GNPs with the addition of a DNA repair inhibitor, the DNA damage in cancer cells can be further enhanced causing more cell death. Pyronaridine (PYD), an antimalarial drug, is being proposed as a potential DNA repair inhibitor. The objective of this research is to examine whether the introduction of PYD into gold-bearing cancer cells will further increase the radiation response. HeLa and HCT-116 cell cultures were dosed with 500 nM of PYD and 7.5 $\mu\text{g/mL}$ of GNPs (~11 nm core diameter functionalized with PEG and a RGD peptide). Cell cultures were irradiated with 2 Gy using a clinical 6 MV linear accelerator. Different dosing conditions were compared to examine the enhancement of DNA damage in cells treated with PYD and GNPs. Cellular damage was analyzed using a cell proliferation assay and a DNA double-strand breaks (DSBs) assay. The results showed that with a radiation dose of 2 Gy, there was a 42% increase in DNA DSBs in HeLa cells that were treated with PYD and GNPs versus cells treated solely with GNPs. Qualitative data for HCT-116 displayed an increase in DSBs with the combined approach. Furthermore, this outcome was supported as data showed that there was a significant decrease in cell proliferation 24 hours after radiation for both cell lines dosed with the combination of GNPs and PYD versus solely GNPs. We have shown that PYD can be used to further increase the efficacy of the combined therapeutic approach of radiotherapy and GNPs to combat cancer. This is very promising as this novel approach could offer significant therapeutic benefits in the clinic. The GNPs used in our study have already been tested in phase I trials, and with PYD being a clinically approved drug, the transition of this combined modality into radiotherapy treatment is feasible.

This work was supported by Nanomedicines Innovation Network (NMIN) Strategic Initiative (SI) grant, 2021-RES-SI-05; Natural Sciences and Engineering Research Council (NSERC) Discovery Grant (DG), RGPIN-2017-04501; Kuwait Foundation for the Advancement of Sciences (KFAS), CB21-63SP-01; Canadian Institute for Health Research (CIHR), CIHR PJT-399879; and Alberta Cancer Foundation Transformative Program Project, 26603.

Green-solvent-processed conjugated polymers for photovoltaics and optoelectronics

B. Nasrollahi¹, J. M. Jailani¹, V. Pecunia^{1,*}

¹Pecunia Research Group Sustainable Optoelectronics
School of Sustainable Energy Engineering, Simon Fraser University
e-mail: vincenzo_pecunia@sfu.ca

Today organic photovoltaic devices are in an ever-growing demand for a wide range of applications. Organic photovoltaics drew countless attention to their favorable features like spectral tunability, lightweight, flexibility, low cost, and easy processing. However, a key issue in organic optoelectronics and photovoltaics concerns their typical reliance on toxic solvents such as chloroform, chlorobenzene, and 1,2-dichlorobenzene for processing, which poses a serious risk to the environment and human health. Therefore, to address this challenge, eco-friendly processing approaches have been investigated. Here, we discuss the recent strategies developed for replacing the halogenated solvents with the functional non-halogenated solvents referred to as “green solvents” (e.g., xylenes, toluene, and tetrahydrofuran), which are known to be less toxic [1-3]. We also cover additive-based approaches—which involve the dissolution of the photoactive materials in non-halogenated solvents—and the design of the polymer structure to enhance their solubility in green solvents. High-boiling-point solvents selectively dissolving donors or acceptors used alongside solvent additives have shown promising results. Solar cell efficiency of more than 16% has been achieved by using 1,8-diiodooctane (DIO) in toluene [4]. Moreover, a considerable advance in solar cell efficiency was obtained by modulating the molecular structure PM6:Y6 counterparts: by engineering Y6 into DTY6, the solar cell efficiency was increased from 10.8% to 16.1% while using ortho-xylene as the green solvent [1]. Finally, we summarize the recent developments aiming at truly green processing by using water and alcohol as solvents [1],[3]. The best water-processed nanoparticle system showed a high efficiency of 11% with DIO as a solvent additive [5]. These results highlight that significant progress has been achieved in engineering green-solvent-processed polymer semiconductors toward efficient photoconversion. However, these efficiencies are yet to reach levels on par with conventionally processed polymer devices, hence further efforts are needed to realize their full potential.

References

- [1] S. Lee, D. Jeong, C. Kim, C. Lee, H. Kang, H.Y. Woo, and B. J. Kim, *ACS Nano*, **14**, 14493-14527 (2020).
- [2] C. Larsen, P. Lundberg, S. Tang, J. Ràfols-Ribé, A. Sandström, E. Mattias Lindh, J. Wang, and L. Edman, *Nature Communication*, **12**, 1-7 (2021).
- [3] S. Zhang, L. Ye, H. Zhang, and J. Hou, *Materials Today*, **19**, 553-543 (2016).
- [4] L. Hong, H. Yao, Z. Wu, Y. Cui, T. Zhang, Y. Xu, R. Yu, Q. Liao, B. Gao, K. Xian, H. Y. Woo, Z. Ge, and J. Hou, *Advanced Materials*, **31**, 1903441 (2019).

3D Bioprinting Human Models of Parkinson's Disease

Ruchi Sharma¹, Milena Restan², Kali Scheck³ and Stephanie Willerth^{1,2,3*}

¹Department of Mechanical Engineering, University of Victoria, Victoria, BC V8W 2Y2, Canada;
ruchis0983@gmail.com

²Department of Biomedical Engineering, University of Victoria, Victoria, BC V8W 2Y2, Canada;

³Division of Medical Sciences, University of Victoria, Victoria, BC V8W 2Y2, Canada;

* Correspondence: willerth@uvic.ca; Tel.: +1-250-721-7303

Parkinson's disease (PD), a prolonged, chronic neurodegenerative disorder, results from the progressive loss of nigrostriatal dopaminergic neurons (DNs) which are necessary for voluntary motor control. Somatic cells (skin or blood cells) from PD patients with mutations may be reprogrammed using transcription factors to human induced pluripotent stem cells (hiPSCs) [1]. These hiPSC lines from patients can then be differentiated into DNs to imitate PD. Here, 3D structures were bioprinted using PD patient-specific neural progenitor cells (NPCs) encased within a bioink containing drug-releasing microspheres. HiPSC-derived NPCs were primed for 7 days prior to printing with FGF-8 (100ng/ml) and Purmorphamine (2uM). These NPCs were printed with bioink containing guggulsterone encapsulated microspheres with Aspect Biosystems' RX1 bioprinter [1,2]. These constructs were then cultured, and their characteristics were studied, including their morphology, cell death, and alpha-synuclein aggregation. Further, neural induction medium was used to differentiate bioprinted NPCs for 20 days before BrainPhys media was added for an additional 10 days of maturation. The generated tissues had over $88.2 \pm 1.5\%$ cellular viability one day after printing, which increased to $96.7 \pm 1.8\%$ on day seven. After 20 days, tissues were stained for early neuronal markers such FOXA2 (Forkhead box protein A2) and TUJ1 (beta-tubulin III). However, in addition to neuronal markers, these tissues also showed expressions of the PD-specific markers alpha-synuclein, DJ-1 (Protein Deglycase DJ-1), and LRRK2 (Leucine Rich Repeat Kinase 2). These bioprinted humanized PD models might be studied to better understand the disease's pathogenesis. These studies suggest that 3D bioprinting is necessary in order to produce complex 3D models.

Acknowledgement: The authors acknowledge funding from CIHR Project grant, NSERC Discovery Grant, CRC program.

References

- [1] Gonzalez, R., et al., Deriving dopaminergic neurons for clinical use. A practical approach. *Sci Rep*, 2013. **3**: p. 1463.
- [2] Sharma, R., et al., 3D Bioprinting Pluripotent Stem Cell Derived Neural Tissues Using a Novel Fibrin Bioink Containing Drug Releasing Microspheres. *Frontiers in Bioengineering and Biotechnology*, 2020. **8**(57).

Investigating polymer growth via 4D STEM-in-SEM

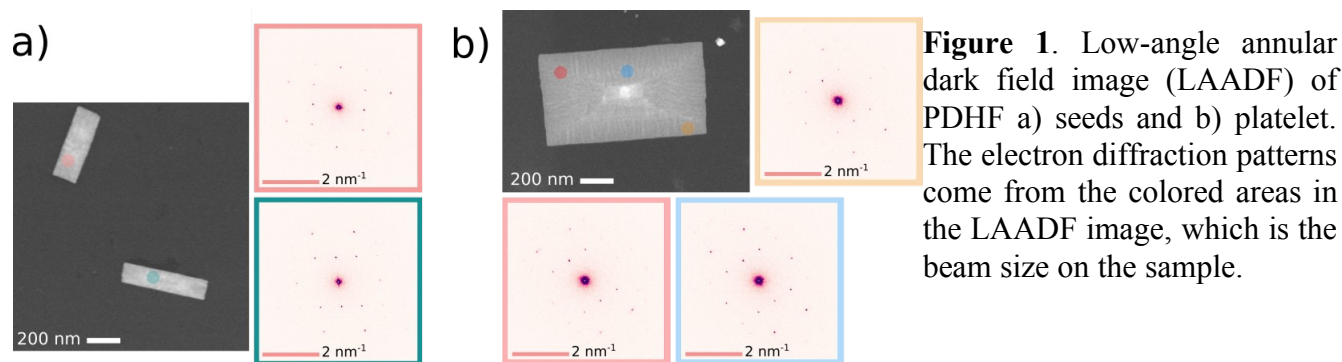
C. Cordoba^{1,2}, S. Lei,² I. Manners², A. Blackburn^{1,2}

¹University of Victoria, Department of Physics and Astronomy, Advanced Microscopy Facility

²University of Victoria, Department of Chemistry

e-mail: cccordoba@uvic.ca

Organic compounds offer various advantages in terms of cost and property tunability in the manufacturing of standalone optoelectronic devices, as well as to those complementary to inorganic technologies [1]. Self-assembled amphiphiles and molecules in solution allow for the synthesis of corona-core nanoparticles with nanostructures that are uniform, supporting long exciton diffusion lengths [2]. The characterization of these soft nanostructures via electron microscopy is challenging due to the ionization and breakage of chemical bonds by the electron beam, as well as other undesirable effects like crosslinking, crystallinity loss and heat generation [3]. Scanning Electron Microscopy (SEM) in conjunction with segmented scanning transmission electron microscopy (STEM) detectors can overcome some of these challenges as they operate at lower voltages (5-30 eV). Furthermore, by using high-speed direct electron detectors in what is known as four-dimensional (4D) STEM-in-SEM, one can access diffraction information at lower electron-dose and high-throughput, crucial to understanding structure and growth in these sensitive materials. In this contribution, we studied one- and two-dimensional (1D and 2D) structures formed from the self-assembly of block copolymers and homopolymers, respectively, consisting of crystallizable polyferrocenylsilane (PFS) and poly(di-n-hexylfluorene) (PDHF) segments (Fig. 1). Experimental data was acquired using a Hitachi SU9000 SEM and Hitachi High-Technologies Canada's Azorus software to control, acquire and inspect data from a Dectris Quadro pixelated hybrid direct electron detector camera. The microscope operated in low magnification mode at 20 keV to give a beam current of 1.62 nA and convergence semi-angle of about 0.2 mrad. We estimated that the sample received an exposure dose of less than 2 e-/Å², while positioning the sample. 4D-STEM data was acquired over a 21 × 21 μm field of view (FOV) in sets of 30 × 30 to 100 × 100 square grid patterns, resulting in 900 to 10000 diffraction patterns (DPs). DPs had exposure times of 20 and 10 ms, resulting in average electron doses of ~17 to 25 e-/Å².



References

- [1] O. S. Serbanescu, S. I. Voicu, V. K. Thakur, *Materials Today Chemistry*, **17**, 1- 43, (2020).
- [2] X. H. Jin, M. B. Price, J. R. Finnegan, C. E. Boott, J. M. Richter, A. Rao, S. M. Kenke, R. H. Friend, G. R. Whittell and I. Manners, *Science*, **360**, 897-900, (2018).
- [3] G. H. Michler, *Problems Associated with the Electron Microscopy of Polymers*. (n.d.). In *Electron Microscopy of Polymers*, Springer Berlin Heidelberg, (2008).

A New Method for Measuring the Ionic Conductivity of Solid Polymer Electrolyte Powders

Ana Laura G. Biancolli, Anastasiia Konovalova, Steven Holdcroft

Holdcroft Research Group, Department of Chemistry, Simon Fraser University, 8888 University Drive, Burnaby.
e-mail: ana_laura_goncalves_biancolli@sfu.ca

Emerging ion conducting polymers require a comprehensive set of characterizations to determine compatibility with prospective applications. The determination of the ionic conductivity of materials is crucial as this property influences the performance of electrochemical energy conversion devices. Normally, the characterization of transport phenomena is primarily performed on thin membrane form of the polymers. However, not all newly synthesized materials can be fabricated into free-standing films and only exist in their powder form¹. Moreover, solid polymer electrolytes (SPE) powders are gaining attention as additives to catalyst layers to enhance the transport of ions^{2,3}. A technique capable of measuring precisely the ionic conductivity of powder polymers under different conditions (temperature and relative humidity) is thus essential to will assist fine-tuning of synthetic routes of ionic polymers during early stages of the material development. In the absence of a suitable technique, our research group has explored a new method of measuring the ionic conductivity of polymers in powder form. The novel methodology uses a modified through-plane cell from Scribner Associates and the Membrane Test System MTS-740 coupled to a Solartron Analytical 1260 Impedance Analyzer to measure the ionic resistance of powders. Two types of SPEs were used in this study: a proton-exchange SPE powder (H⁺ form) and an anion-exchange SPE powder (Cl⁻ form). The materials were hard-pressed into rectangular pellets to allow the assembly in the MTS-740 through-plane cell. The experimental results reveal that it is possible to measure the ionic resistance of proton-exchange SPE pellets having different thicknesses with consistent conductivity values through the variation in thickness. The new method allows access to higher conductivity values than those measured by a conventional through-plane glass cell¹; e.g. 210 vs 130 mS cm⁻¹, respectively, for proton-exchange SPE powder at 80 °C and 95 % RH (MTS-740 cell) or fully humidified (conventional glass cell), and 53 vs 24 mS cm⁻¹, respectively, for anion-exchange SPE powder at 80 °C and 95 % RH (same condition for both cells). These differences are due to the geometry of the MTS-740 cell that grant easy access to water vapor, in addition to the four-terminal configuration used for the EIS measurements that provide more accurate results than two-terminal sensing. Using this new method, it was possible to record the resistance of SPE powders as a function of relative humidity and temperature, and to collect values above the boiling point of water by applying back pressure to the system, which is especially relevant given emerging applications of high temperature alkaline fuel cells.

This work was supported by the Natural Sciences and Engineering Research Council of Canada (NSERC) through Alliance Grant ALLRP 570797–21. ALGB acknowledges FAPESP grants No. 2019/26955-3 and 2021/14786-2.

References

- [1] Balogun, E., Cassegrain, S., Mardle, P., Adamski, M., Saatkamp, T., & Holdcroft, S. *ACS Energy Letters*, **7(6)**, 2070–2078 (2022);
- [2] Poynton, S. D., Slade, R. C. T., Omasta, T. J., Mustain, W. E., Escudero-Cid, R., Ocón, P., & Varcoe, J. R. *Journal of Materials Chemistry A*, **2(14)**, 5124–5130 (2014);
- [3] Gonçalves Biancolli, A. L., Herranz, D., Wang, L., Stehlíková, G., Bance-Soualhi, R., Ponce-González, J., Ocón, P., Ticianelli, E. A., Whelligan, D. K., Varcoe, J. R., & Santiago, E. I. *Journal of Materials Chemistry A*, **6(47)**, 24330–24341 (2018).

Sub-Ångström Imaging in a Scanning Electron Microscope at 20 kV

Arthur M. Blackburn^{1,2,*}, Cristina Cordoba^{1,2}, Matthew Fitzpatrick^{1,2}, Robert McLeod³

¹ Department of Physics and Astronomy, University of Victoria

² Centre for Advanced Materials and Related Technologies, University of Victoria

³ Hitachi High-Tech Canada Inc., Etobicoke ON, M9W 6A4, Canada.

*e-mail: ablackbu@uvic.ca

Advances in electron microscopy techniques and instrumentation aim to maximize the useful information obtained from sample observations while minimizing the time and cost of the study. With this goal there has been a long-standing desire to obtain high spatial resolution ($< 10^{-10}$ m, sub-Ångström) sample information from general purpose, non-aberration corrected, low energy (< 30 keV) scanning electron microscopes (SEMs). Here we experimentally show a resolution of at least 0.7 Å with a 20 keV electron beam operating in a transmission mode within this class of SEM, thus realizing this goal. We achieve this through combination of multiple advances: adding a simple diffraction projector lens to the microscope; using un-coated hybrid direct electron detector; and incorporating calibration and correction of diffraction data pincushion distortion within a multi-slice ptychographic reconstruction algorithm. Furthermore, we see that employment of background correction routines, which hitherto have not been applied to electron ptychography, allow the determination of $< 10^{-10}$ m information in few-layer materials such as gold – MoS₂ heterostructures in the presence of surface contamination at 20 keV. While our 0.7 Å resolution measure is given from a standard Fourier ring correlation treatment of reconstructions of gold particles on amorphous carbon (such as shown in Fig. 1), simple Fourier analysis of imaged gold - MoS₂ structures indicates the presence of 0.6 Å features. The resulting images compare well to aberration corrected TEM imaging performed at much higher (≥ 60 keV) beam energies. These advances allow the acquisition of high-resolution, sub-Ångström information from beam sensitive materials that hitherto could only be obtained in specialized aberration corrected transmission electron microscopes operating with much greater beam energies.

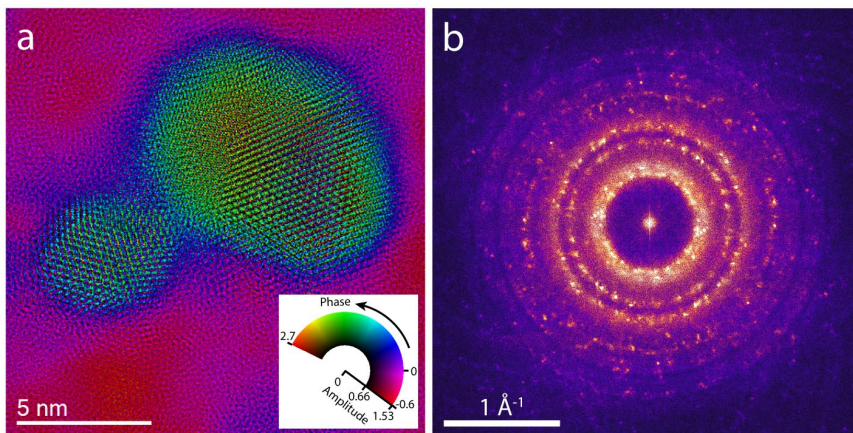


Figure 1 – (a) Reconstructed exit wave for electron transmission through a gold particle supported on thin carbon imaged at 20 keV and (b) a fast Fourier transform of multiple reconstructed gold particle images.

This work was funded by NSERC and Hitachi High-Tech Canada within a Collaborative Research and Development project.-

Slow Spontaneous Enhancement in Efficiencies of Single-Crystal Lead Halide Perovskite Solar Cells

Vishal Yeddu^{1,3}, Parinaz Moazzezi^{2,3}, Bekir Turedi⁴, Muhammad N. Lintangpradipto⁴, Dongyang Zhang^{1,3}, Soumya Kundu^{1,3}, Deepak Thrithamarassery Gangadharan^{1,3}, Reuven Gordon^{2,3}, Osman M. Bakr⁴, Makhsud I. Saidaminov^{1,2,3*}

¹University of Victoria, Department of Chemistry

²University of Victoria, Department of Electrical and Computer Engineering

³University of Victoria, Centre for Advanced Materials and Related Technologies

⁴King Abdullah University of Science and Technology, Division of Physical Science and Engineering
e-mail: msaidaminov@uvic.ca

Perovskite solar cells (PSCs) using metal halide perovskites as a photoactive layer have been the subject of extensive research in the photovoltaic community due to their excellent optoelectronic and charge carrier properties. In just over a decade, the highest certified power conversion efficiency (PCE) of PSCs has increased from 3.9% in 2009 to 25.7% in 2022. This is remarkable because it took around 50 years of research and development to increase the efficiency of conventional silicon based solar cells over 25%.

Currently, most efficient PSCs are based on polycrystalline thin films. However, substantial structural disorder and defective grain boundaries place a limit on their performance. Perovskite single crystals are free of grain boundaries, leading to significantly low defect densities, and thus hold promise for high-efficiency photovoltaics. For mature photovoltaic technologies such as Si, GaAs and CdTe, the efficiencies of single-crystal solar cells surpass the efficiencies shown by their polycrystalline counterparts. This is expected as single-crystal films have lower trap densities than polycrystalline films due to the absence of grain boundaries. We, therefore, work on improving the PCE of single crystal PSCs.

Here, we investigate the slow spontaneous enhancement in PCE observed in single crystal methylammonium lead iodide PSCs. Spontaneous enhancement refers to the phenomena by which the PCE increases automatically with aging. We show that the average PCE of 5 SC-PSCs increases by at least 50% upon storage in an inert atmosphere for two weeks. We found out that the interface-trapped solvent which slowly escapes upon aging is responsible for the spontaneous efficiency enhancement in single crystal PSCs.

This work was supported by Solaires Enterprise Inc., Canadian Natural Sciences and Engineering Research Council (NSERC) (ALLRP 566552 - 21), NSERC (RGPIN-2020-04239), the Canadian Foundation for Innovation (40326), and the Canada Research Chairs Program (CRC-2019-00297).

Visualization of Hydroxide Ion Formation upon Electrolytic Water Splitting in an Anion Exchange Membrane

X. Cao¹, D. Novitski¹, S. Holdcroft

¹Simon Fraser University, Department of Chemistry

e-mail: holdcrof@sfu.ca

Measurement of hydroxide ion conductivity is paramount to understanding anion exchange membranes (AEM) operated under alkaline conditions, but the measurement is complicated by dissolved CO₂ and the presence of bicarbonates and carbonates. A technique for accurate measurement has recently been reported that involves measuring the conductivity during water splitting, wherein hydroxide ions are assumed, but not proven, to be produced at the cathode and which purge out other anions. In this preliminary study, we visualize the formation of hydroxide ions and their diffusion from the cathode to anode. We do this by way of an anion exchange membrane cast with an acid/base pH indicator, such that visual confirmation of hydroxide production at the cathode is obtained during application of sustained current load. This proof of concept is demonstrated using the AEM, hexamethyl-p-terphenyl poly(methylbenzamidazolium), and pH indicator, thymolphthalein and acid fuchsin.

This work was supported by Natural Sciences and Engineering Research Council of Canada (NSERC).

References

- [1] Cao, X., Novitski, D. & Holdcroft, S. Visualization of Hydroxide Ion Formation upon Electrolytic Water Splitting in an Anion Exchange Membrane. ACS Mater. Lett. 1, 362–366 (2019).
- [2] Ziv, N. & Dekel, D. R. A practical method for measuring the true hydroxide conductivity of anion exchange membranes. Electrochem. commun. 88, 109–113 (2018).
- [3] Wright, A. G. et al. Hexamethyl-P-terphenyl poly(benzimidazolium): A universal hydroxide conducting polymer for energy conversion devices. Energy Environ. Sci. 9, 2130–2142 (2016).

Control of release kinetics of small molecules from a supramolecular gel

Nikoo Rahbari Asr^{a,b} and Cornelia Bohne^{a,b*}

^a *Department of Chemistry, University of Victoria, PO Box 3065, Victoria, BC, V8W 3V6, Canada.*

^b *Centre for Advanced Materials and Related Technology (CAMTEC), University of Victoria, 3800 Finnerty Rd, Victoria, BC, V8P 5C2, Canada.*

e-mail: Nikoo.rahbari@gmail.com

Hydrogels have been used by many scientists in controlled-release drug delivery systems. Due to their generally favorable biocompatibility, polymeric hydrogels have been an interest for biomaterials applications for a long time. However, because they need covalent crosslinking, drug loading efficiency is low and time-consuming. As a result, a delivery system in which gelation and drug loading can occur together in an aqueous environment and without covalent crosslinking would be attractive. Supramolecular hydrogels have the described characteristic.

The overall project that I aim to do, is using a supramolecular hydrogel as a carrier of two different guests which will be localized in the immobile phase of the gel based on their hydrophobicity and complexation with macrocycles and study the effect of binding and complexation on the release kinetic of these guests. Therefore, cucurbituril will be used as a host. Cucurbiturils are symmetrical structural host with different size of the cavity and solubility in water. They are not only toxic, but also protect the guest from degradation. Sodium deoxycholate is a bile salt which is capable of making supramolecular gels. This investigation will determine the effect on the release profile of each guest with the addition and complexation of the two macrocycles, CB[6] and CB[7].

Studies shows that the release and diffusion of the guest is not just affected by the strength of the gel and molecular level interaction. Most of the work that has been done to improve the release kinetics in literature has focused on improving the swelling, diffusion or degradation behavior of the carrier. However, based on the previous studies in our group⁴ binding of the small molecules(guest) to the gel and localization of the guest (drug model) to the system also plays a role and for different guests, the release profile is not the same and for some of them the percentage of released dye is smaller in the same time scale. Hence, what I am trying to do is studying the variables that would affect the release kinetics for different guests to increase the possibility of having a desired and selective release profile for a specific guest.

Numerical Simulation of Tri-Layers Conducting Polymer Actuators

Erfan Taatizadeh¹, Freya Hik¹, Saeedeh Ebrahimi Takalloo², John D. W. Madden^{1,2}

¹ School of Biomedical Engineering, The University of British Columbia, Vancouver, Canada

² Department of Electrical and Computer Engineering, The University of British Columbia, Vancouver, Canada

e-mail: erfan.taatizadeh@ubc.ca

Abstract:

Tactile feedback plays a vital role in the human sensory perception to acquire information from the outside world [1] and can be found in several forms including vibrotactile, shape, texture, and force feedback. Among those, vibrotactile feedback has been shown to be a highly effective stimulating method of the largest sensory organ, the skin. Hence, it could be used to reproduce texture, generate contact forces, relay information, and more [2]. A man-made tactile feedback actuator as an external stimuli generator device aims to produce mechanical strain and force within a detectable skin sensory range. One of the novel vibrotactile technologies is conducting polymers (CP) actuators. They can be operated with safe and accessible voltages to drive thin, compliant haptic devices. Along with their low-cost fabrication, being lightweight, and high mechanical deformability, they also promise low energy consumption. However, this technology has not yet been explored to a great extent including their engineering foundation along with their operation principles [3]. Actuation performance, durability, and effective fabrication are some aspects that are still obstacles to a successful. When CP actuators are operated in frequency mode, there is always a roll-off in mechanical response due to various rate-limiting factors. However, optimal sensitivity is achieved at frequencies between 150 and 300 Hz – a frequency range that is difficult to reach in CPs due to a drop in generated displacement and force at high frequencies. In addition, the dimension of the tri-layer actuators affects the mechanical outputs. The thicker tri-layer actuators lead to a higher generated force at a cost of low mechanical strain while the longer ones result in a lower generated force and a higher displacement amplitude. In essence, this trade-off between these two plays a vital role in the skin detectability and hence, the efficiency of our proposed haptic technology. Simulation can be used as a valuable tool to decide on the optimized material properties used in the device, the device dimension, and operating conditions, prior to the device's fabrication, to target the required force, displacement, and response time. In this work, we demonstrate the physics-based finite element analysis (FEA) numerical simulation of such tri-layers CP actuators. The novelty of this simulation compared to the previous works is its comprehension: it includes electrical resistance, electrochemical, electro-chemo-mechanical, and inertial effects (mass and damping effects of the device) which paves the way to complete device modeling. Frequency responses match in amplitude from 0.01 to 100 Hz, including resonance frequency. Guided by simulations, already a fivefold increase in the displacement of conducting polymer actuators in a region close to the natural frequencies (~50 Hz) is observed, and guided by simulations, the aim is to show large displacements and forces up to 150 Hz.

References

- [1] S. Choi and K. J. Kuchenbecker, "Vibrotactile display: Perception, technology, and applications," *Proc. IEEE*, vol. 101, no. 9, pp. 2093–2104, 2012.
- [2] V. Hayward and M. Cruz-Hernandez, "Tactile display device using distributed lateral skin stretch," presented at the Proceedings of the haptic interfaces for virtual environment and teleoperator systems symposium, 2000, vol. 69, no. 2, pp. 1309–1314.
- [3] Y. Bar-Cohen and I. A. Anderson, "Electroactive polymer (EAP) actuators—background review," *Mech. Soft Mater.*, vol. 1, no. 1, pp. 1–14, 2019.

Fabrication of Efficient and Stable Perovskite Solar Cells in Ambient Air

Muhammad Awais¹, Deepak T. G.², Furui Tan⁴ and Makhsud I. Saidaminov^{1,2,3*}

¹University of Victoria, Department of Electrical and Computer Engineering

²University of Victoria, Department of Chemistry

³Centre for Advanced Materials and Related Technologies (Times New Roman 11, centered)

⁴Key Laboratory of Photovoltaic Materials, Henan University, Kaifeng, 475004, P. R. China

e-mail: msaidaminov@uvic.ca

The performance of perovskite solar cells (PSCs) has seen rapid growth in about a decade due to the meticulous optimization of device fabrication procedures and material compositions. Most reports focus on device fabrication protocols in an inert atmosphere. Only a few offer reproducible methods to fabricate PSCs in ambient air, and even fewer report stable maximum power point (MPP) operation of devices. This protocol work presents detailed protocols for fabricating 20% milestone PSCs in ambient air and their encapsulation toward stable 500+ hrs MPP operation. We also developed a simple encapsulation testing protocol: we found that if an encapsulated device withstands 120°C heat stress for 5 minutes in ambient air, it likely withstands long-term MPP conditions.

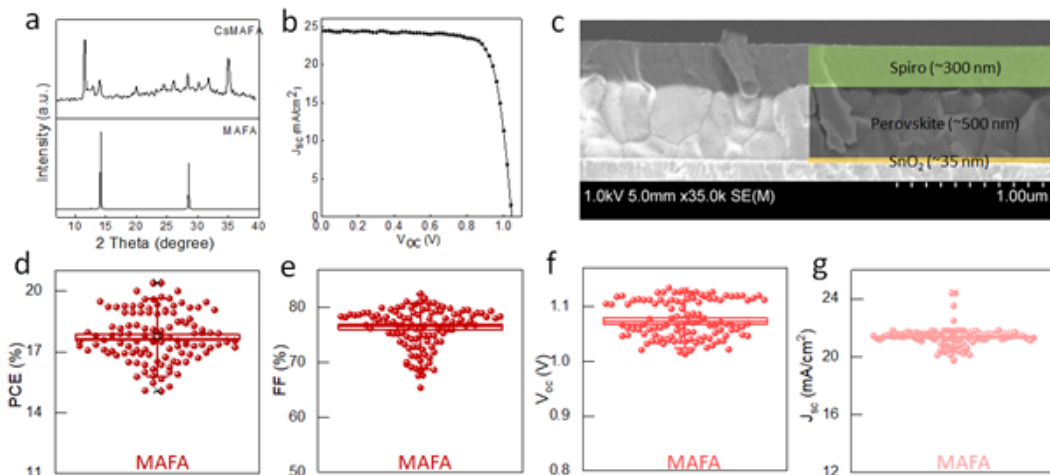


Figure 1. Characterization of perovskite films and solar cells. (a) XRD spectra of perovskite films; (b) IV curve of the champion cell; (c) Cross-sectional SEM image of the perovskite solar cell; (d) PCE, (e) fill factor (FF), (f) open-circuit voltage (V_{oc}) and (g) short-circuit current (J_{sc}) for over 100 perovskite solar cells fabricated in ambient air.

We thank Solaires Entreprises Inc. and Canada's Natural Sciences and Engineering Research Council (ALLRP 561355 - 20) for their financial support. M.I.S. is grateful to the NSERC (RGPIN-2020-04239), the Canadian Foundation for Innovation (40326), and the Canada Research Chairs Program (CRC-2019-00297) for financial support. We thank Mark Evens for devising the LED-based MPP station.

References

- [1] Saliba, M. *et al.* How to Make over 20% Efficient Perovskite Solar Cells in Regular (n-i-p) and Inverted (p-i-n) Architectures. *Chemistry of Materials* **30**, 4193–4201 (2018).

Optimization of Electric Field-Directed Chaining of Nanowires Using Non-Polar Solvent and External Magnetic Field

M. Y. Arafat^{1,2}, M. Xu^{1,2}, R. Bhiladvala^{1,2,3*}

¹University of Victoria, Department of Mechanical Engineering

²Centre for Advanced Materials and Related Technologies

³Integrated Energy Systems at the University of Victoria

e-mail: rustomb@uvic.ca

Nanowire-based transparent electrodes are of great interest for small-scale sensors and large-area displays. Aligning nanowires (NWs) in an ordered network applying external forces requires several parameters to consider and is thus challenging to achieve. Electric field-directed chaining in a nanowire (NW) suspension has been demonstrated as a simple cost-effective process for large area coverage with high conductivity and transparency. But the generation of an effective dielectrophoretic (DEP) force for desired NW assembly requires a high frequency to overcome the effect of an electrical double layer arising from the polarity of water used as a solvent. Moreover, the magnitude of the electric field falls dramatically in the region away from the electrodes. Herein, we propose the use of squalane (C₃₀H₆₂), a relatively non-polar and non-toxic liquid compared to existing solvents, as a potential candidate for NW suspension in a field-directed assembly. Theoretical analysis shows that squalane can generate effective DEP force for chaining at a lower frequency because of its low electrical conductivity and dielectric constant. Additionally, the high viscosity of squalane may suppress Brownian motion of NWs and electroosmotic (EO) velocity of the medium, thereby facilitating the chaining process. Finally, we use electromagnetic simulation results to explore how combining an external magnetic field with the electric field may enable better control of the NW assembly far from the electrodes.

This work was supported by a CRD grant from NSERC, and equipment grants from CFI/BCKDF.

Zinc oxide nanowires as qubits

Shirin Riahi¹, Colton Lohn¹, David Lister¹, Maria Viitaniemi², Kai-Mei Fu², Simon Watkins¹

¹ Department of Physics, Simon Fraser University,

² Department of Physics, University of Washington, Seattle

e-mail: simonw@sfu.ca

Zinc oxide has been investigated for several decades due to its direct bandgap, and relative ease of n-type doping. The bandgap is close to that of GaN, which has led to intense efforts to develop near UV light emitters. This work has been stalled due to the lack of suitable p-type dopants. Among the commonly investigated compound semiconductors ZnO has the lowest spin orbit coupling. This has recently been shown¹ to result in long spin lattice relaxation times T_1 for donor spins compared with other compound semiconductors. Zinc oxide nanowires are a promising platform for the study of single donor spins. In this poster we present results of our efforts at SFU to grow undoped and Ga-doped ZnO nanowires and implement these structure in quantum control experiments. We use donor spins localized at shallow donor impurity sites. At low temperature donor bound excitons (D^0X) are in turn bound to these donors and offer the possibility of optical pumping via a lambda transition approach. One of the factors limiting spin lattice relaxation and spin coherence is the spectral width of the optical peaks due to impurity-related inhomogeneous broadening. Through intentional donor doping we have investigated possible inhomogeneous broadening mechanisms based on (1) donor pair tunneling (2) Stark effect. These data indicate that we can dope our NWs with substitutional donors down to around 10^{16} cm^{-3} .

Attempts to fabricate free standing NWs for quantum information studies using selective area growth were attempted but proved difficult due to poor selectivity with respect to the masking materials (SiO_2 and SiN). As a first attempt at measuring spin properties NWs were removed from the substrate and placed by drop-casting onto a substrate. Confocal microscopy was performed on single NWs such that on average 1000 donor spins were imaged. Optical pumping measurements of specific donor spin orientations showed significant improvements for single NW compared with ensemble NW measurements. Inhomogeneously broadened linewidths of 50 GHz were observed by photoluminescence excitation spectroscopy. Two laser excitation measurements resulted in the appearance of a 2 GHz linewidth dip in the main luminescence peak due to coherent population trapping, confirming the suitability in principle of this system for quantum information applications.^{2,3}

Acknowledgement:

The support of the Natural Sciences and Research Council of Canada is gratefully acknowledged

References

- [1] X. Linpeng, T. Karin, M. V. Durnev, R. Barbour, M. M. Glazov, E. Ya. Sherman, S. P. Watkins, Satoru Seto, and Kai-Mei C. Fu, Phys. Rev. B **94**, 125401 (2016)
- [2] Xiayu Linpeng, Maria L.K. Viitaniemi, Aswin Vishnuradhan, Y. Kozuka, Cameron Johnson, M. Kawasaki, and Kai-Mei C. Fu, Phys. Rev. Applied **10**, 064061 (2018)
- [3] M. L. K. Viitaniemi, Christian Zimmermann, Vasileios Niaouris, Samuel H. D'Ambrosia, Xin Wang, E. Senthil Kumar, Faezeh Mohammadbeigi, Simon P. Watkins, and Kai-Mei C. Fu, Nano Letters **22** 2134 (2022)